Ligand Elaboration Mediated by a Cp*W(NO) Template: Stepwise Incorporation of Small Molecules into a Tungsten Vinyl Fragment

Peter Legzdins* and Sean A. Lumb

Department of Chemistry, The University of British Columbia, Vancouver, British Columbia, Canada V6T 1Z1

Victor G. Young, Jr.[†]

Department of Chemistry, The University of Minnesota, Minneapolis, Minnesota 55455

Received December 9, 1997

Thermolysis of the alkyl vinyl complex Cp*W(NO)(CH$_2$SiMe$_3$)(CPh=CH$_2$) (**1**) in the presence of unsaturated, heteroatom-containing compounds such as esters and nitriles quantitatively affords metallacyclic products of reductive coupling. These are trapped as 18e complexes via either intramolecular rearrangement or intermolecular reaction with added trapping reagents. The nature of these metallacycles is consistent with the intermediacy of the acetylene complex Cp*W(NO)(η^2-CPh≡CH) (**A**) derived in situ from the reductive elimination of SiMe$_4$ from **1**. With esters ROAc (R = Me, Et), reductive coupling and C−O bond cleavage yields the alkoxide-containing oxametallacyclopentadiene complexes Cp*W-(NO)(η^2-*O*=C(Me)CH=*C*Ph)(OR) (**2**, R = Me; **3**, R = Et). Thermolysis of **1** in RCN (R = Me, Et, ^{i}Pr) containing small excess amounts of R′OH yields the respective hydroxide or alkoxide compounds Cp*W(NO)(η^2-*N*H=C(R)CH=*C*Ph)(OR′) (**4**, R = Me, R′ = H; **5**, R = Et, R′ = H; **6**, R = ^{i}Pr, R′ = H; **7**, R = Me, R′ = C$_3$H$_5$). Utilization of cyclopentadiene (CpH) as the trapping agent in MeCN affords the aminopentafulvene complex Cp*W(NO)(HNC(=C(C$_4$H$_4$))-(Me))(η^2-*N*H=C(Me)CH=*C*Ph) (**8**). VT ^{1}H NMR spectroscopy reveals the fluxional solution behavior of the fulvene ligand in **8**. Thermolysis of **1** in RCN (R = Me, ^{i}Pr) containing trace amounts of acetone gives the bicyclic species Cp*W(NO)(η^3-*O*C(Me)$_2$*N*=C(Me)CH=*C*Ph) (**9**, R = Me; **10**, R = ^{i}Pr). In the absence of added trapping reagent, thermolysis of **1** in RCN (R = Me, Et) yields the vinyl amidinate complexes Cp*W(NO)(η^3-*N*HC(R)=*N*C(=C(R^1)(R^2))-CH=*C*Ph) (**11**, R = Me, R^1 = R^2 = H; **12**, R = Et, R^1 = H, R^2 = Me). The molecular structures proposed for **2**, **4**, **8**, and **10** are confirmed by single-crystal X-ray analyses. Mechanistic proposals to account for the observed chemistry are corroborated by the results of labeling studies, while a kinetic study of the transformations yielding **3**, **4**, and **11** implicates the rate-limiting generation of acetylene intermediate **A**. A qualitative orbital overlap rationale is proposed to account for the observed chemistry.

Introduction

Of fundamental importance is the bond-forming process involving the coupling of two unsaturated substrates. That a transition metal (TM) environment possesses the ability to act as a template for such bond formation represents one of the most significant applications of modern organotransition metal chemistry.[1] Since the first report of Ni-induced alkyne cyclotrimerization,[2] TM-induced reductive coupling of unsaturated organic substrates has provided access to a wealth of polyfunctional cyclic hydrocarbons and heterocycles.[3]

* To whom correspondence should be addressed.

† To whom correspondence regarding X-ray crystallographic analyses should be addressed.

(1) Collman, J. P.; Hegedus, L. S.; Norton, J. R.; Finke, R. G. *Principles and Applications of Organotransition Metal Chemistry*; University Science Books: Mill Valley, CA, 1987. (b) Crabtree, R. H. *The Organometallic Chemistry of the Transition Metals,* 2nd ed.; Wiley-Interscience: Toronto, 1994.

(2) Reppe, W.; Schlichting, O.; Klager, K.; Toepel, T. *Liebigs Ann. Chem.* **1948**, *560*, 1.

Scheme 1

R = hydrocarbyl
E = C(R″)-, S, NR‴
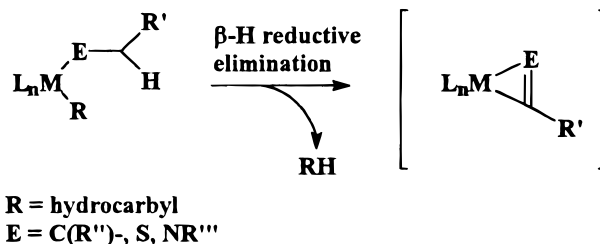
Reductive coupling is typically mediated by TM complexes containing a coordinatively unsaturated, low-valent (electron-rich) metal center, the former charac-

(3) This field has been reviewed extensively, see, for example: (a) Vollhardt, K. P. C. *Acc. Chem. Res.* **1977**, *10*, 1. (b) Buchwald, S. L.; Nielsen, R. B. *Chem. Rev.* **1988**, *88*, 1047. (c) Carnahan, E. M.; Protasiewicz, J. D.; Lippard, S. J. *Acc. Chem. Res.* **1993**, *26*, 90. (d) Broene, R. D.; Buchwald, S. L. *Science* **1993**, *261*, 1696. (e) Negishi, E.-I.; Takahashi, T. *Acc. Chem. Res.* **1994**, *27*, 124.

Scheme 2
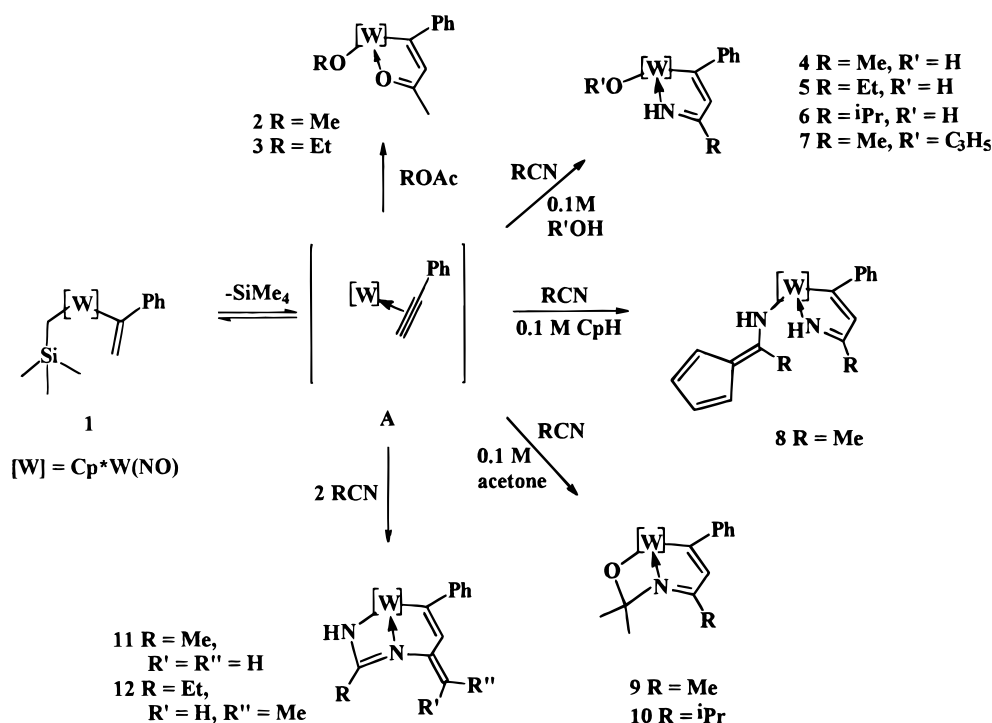
teristic being prerequisite for the initial coordination of unsaturated substrate while the latter is required for the activation of the coordinated substrate toward coupling. While many late transition metal complexes exist in this state and can be manipulated as such, analogous low-valent, "naked" complexes of the early transition metals tend to be unstable and must be generated in situ from higher-valent precursors. A particularly versatile method toward this end involves the in situ reductive elimination of hydrocarbon from a parent hydrocarbyl complex (Scheme 1). Because one of the two unsaturated ligands is generated intramolecularly in the reductive elimination step, the presence of a different unsaturated substrate in the reaction mixture results in products arising from cross-coupling. Further variation can be introduced into the overall reaction by modifying the substituents R′, R″, and R‴ in the parent hydrocarbyl complex.

While current interest in this area spans a number of groups and ligand sets, its foundation is set in the chemistry developed for the group 4 metallocenes.[3b,d,e] Initial reports by Erker described the thermal elimination of benzene from Cp_2ZrPh_2 and proposed the formation of a transient benzyne complex which is capable of coupling to olefins and acetylenes, yielding a plethora of functionalized aliphatic zirconacycles.[4] Buchwald subsequently structurally characterized the phosphine-trapped benzyne complex by X-ray diffraction and extended the reactivity to heteroatom-containing substrates.[5] The method was then generalized so that a variety of alkyne complexes could be obtained through $β$-H reductive elimination of methane from the appropriate methyl alkenyl precursor.[6] The development of this particular methodology involving reductive elimi-

nation of alkane dramatically expanded the range of cyclic and heterocyclic compounds made accessible to the synthetic chemist.

In an earlier communication describing the double C−H activation of *n*-pentane and *n*-hexane,[7] we proposed the formation of $Cp*W(NO)(\eta^2\text{-}PhC≡CH)$ (**A**) by a $β$-H reductive elimination of $SiMe_4$ from $Cp*W(NO)$-$(CH_2SiMe_3)(CPh=CH_2)$ (**1**) under thermolysis conditions in the appropriate hydrocarbon solvent. The structural similarity of **A** to the benzyne complex of Erker and Buchwald prompted us to investigate the reductive coupling chemistry of **A** in the presence of such unsaturated, heteroatom-containing substrates as esters and nitriles, with the expectation that the products of reductive coupling would mirror any orbital differences between the zerovalent $Cp*W(NO)$ template and the isolobal divalent zirconocene analogue. A recent communication reported our preliminary results in this regard.[8] In this paper, we present the full details of this study, including a kinetic analysis of representative reactions, and provide mechanistic evidence and a molecular orbital proposal to account for the chemistry observed. Unlike the group 4 analogues, the group 6 metallacycles initially formed in the reductive coupling event are not isolable as stable, 18-valence-electron (18e) complexes and continue to react, either intramolecularly or with trapping reagents present in the reaction mixture, until electronic saturation is attained.

Results and Discussion

The thermolysis of $Cp*W(NO)(CH_2SiMe_3)(CPh=CH_2)$ (**1**) in the presence of several substituted esters and

(4) (a) Erker, G. *J. Organomet. Chem.* **1977**, *134*, 189. (b) Erker, G.; Kropp, K. *J. Am. Chem. Soc.* **1979**, *101*, 3659.

(5) Buchwald, S. L.; Watson, B. T.; Huffman, J. C. *J. Am. Chem. Soc.* **1986**, *108*, 7411.

(6) (a) Buchwald, S. L.; Lum, R. T.; Dewan, J. C. *J. Am. Chem. Soc.* **1986**, *108*, 7441. (b) Buchwald, S. L.; Watson, B. T.; Huffman, J. C. *J. Am. Chem. Soc.* **1987**, *109*, 2544.

(7) Debad, J. D.; Legzdins, P.; Lumb, S. A.; Batchelor, R. J.; Einstein, F. W. B. *J. Am. Chem. Soc.* **1995**, *117*, 3288.

(8) Legzdins, P.; Lumb, S. A. *Organometallics* **1997**, *16*, 1825.

Table 1. Numbering Scheme, Yield, and Analytical Data for Complexes 2−12

complex	compd no.	color (yield, %)	anal. found (calcd)		
			C	H	N
Cp*W(NO)(OMe)(η^2-*O*=C(Me)CH=*C*Ph)	**2**	purple (89)	47.96 (47.99)	5.09 (5.18)	2.50 (2.67)
Cp*W(NO)(OEt)(η^2-*O*=C(Me)CH=*C*Ph)	**3**	purple (83)	48.77 (49.00)	5.35 (5.42)	2.47 (2.60)
Cp*W(NO)(OH)(η^2-H*N*=C(Me)CH=*C*Ph)·0.5MeCN	**4·0.5MeCN**	orange (84)	47.52 (47.15)	5.27 (5.22)	7.04 (6.60)
Cp*W(NO)(OD)(η^2-D*N*=C(Me)CH=*C*Ph)	**4-d_2**	orange (>95)[a]	[b]		
Cp*W(NO)(OH)(η^2-H*N*=C(Et)CH=*C*Ph)	**5**	red-orange (92)	44.64 (48.99)	5.15 (5.79)	5.12 (5.19)
Cp*W(NO)(OH)(η^2-H*O*=C(iPr)CH=*C*Ph)	**6**	red-orange (83)	48.39 (48.11)	5.57 (5.38)	5.49 (5.34)
Cp*W(NO)(OCh$_2$CH=CH$_2$)(η^2-N*H*=C(Me)CH=*C*Ph)	**7**	red-orange (81)	47.52 (50.20)	5.00 (5.49)	4.65 (5.09)
Cp*W(NO)(HNC(=C(C$_4$H$_4$))(Me))(η^2-H*N*=C(Me)-N(Me)CH=*C*Ph)·MeCN	**8·MeCN**	deep red (75)	54.63 (54.39)	5.75 (5.66)	8.82 (8.75)
Cp*W(NO)(η^3-*O*C(Me)$_2$*N*=C(Me)CH=*C*Ph)	**9**	red-brown (72)	[b]		
Cp*W(NO)(η^3-*O*C(Me)$_2$*N*=C(iPr)CH=*C*Ph)	**10**	red-brown (71)	52.56 (52.92)	5.94 (5.92)	5.01 (4.84)
Cp*W(NO)(η^3-H*N*C(Me)=*N*C(=CH$_2$)CH=*C*Ph)	**11**	dark red (77)	48.90 (49.52)	5.09 (5.10)	6.69 (7.88)
Cp*W(NO)(η^3-D*N*C(CD$_3$)=*N*C(=CD$_2$)CH=*C*Ph)	**11-d_6**	dark red (95)[a]	[b]		
Cp*W(NO)(η^3-H*N*C(Et)=*N*C(=CHMe)CH=*C*Ph)	**12**	red-brown (68)	51.59 (51.32)	5.53 (5.57)	7.55 (7.49)

[a] Yield as indicated in the ^{1}H NMR spectrum of the reaction mixture. [b] Not determined.

Table 2. Mass Spectroscopic Data and IR Spectral Data for Complexes 2−12

compd no.	MS (m/z)[a]	probe temp[b] (°C)	IR (Nujol, cm^{-1})
2	539	200	1532 (ν_{NO})
3	525	150	1538 (ν_{NO})
4	510	150	3562 (ν_{OH})
			1532 (ν_{NO})
4-d_2	512	120	2630 (ν_{OD})
			2282 (ν_{ND})
			1531 (ν_{NO})
5	494 [P$^+$ − NO]	150	3580 (ν_{OH})
			1587 ($\nu_{C=N}$)
			1535 (ν_{NO})
6	508 [P$^+$ − NO]	150	1733 ($\nu_{C=N}$)
			1588 (ν_{NO})
7	550	150	1730 ($\nu_{C=N}$)
			1589 (ν_{NO})
8	599	150	1730 ($\nu_{C=N}$)
			1589 (ν_{NO})
9	550[c]	150	
10	578	150	1598 ($\nu_{C=N}$)
			1542 (ν_{NO})
11	533[d]	80	3268 (ν_{NH})[e]
			1590 ($\nu_{C=C}$)
			1517 (ν_{NO})
11-d_6	539	150	n/a[f]
12	561	150	1598 ($\nu_{C=N}$)
			1529 (ν_{NO})

[a] Values for the highest intensity peak of the calculated isotopic cluster ([184]W). [b] Probe temperatures. [c] High-resolution EI mass spectrum (150 °C), found (calcd): 550.18242 (550.18170), [C$_{23}$H$_{30}$N$_2$O$_2$[184]W, P$^+$]. [d] High-resolution EI mass spectrum (150 °C), found (calcd): 553.16608 (533.16638), [C$_{22}$H$_{27}$N$_3$O[184]W, P$^+$]; 503.16662 (503.16837), [P$^+$ − NO]. [e] KBr pellet. [f] NMR-tube reaction.

nitriles under differing experimental conditions affords the product complexes depicted in Scheme 2. Each reaction portrayed is considered in turn in the following sections. The numbering scheme and analytical data for complexes **2**−**12** are collected in Table 1. Mass and IR spectroscopic data are presented in Table 2. ^{1}H and ^{13}C NMR data for selected compounds are summarized in Table 3, while X-ray crystallographic data for complexes **2**, **4**, **8**, and **10** are given in Table 4.

Reductive Coupling of Esters: Acyl C−O Bond Cleavage. Thermolysis of the red tungsten vinyl complex **1** at 45 °C in the presence of esters such as methyl or ethyl acetate affords the oxametallacyclopentadienyl complexes Cp*W(NO)(OMe)(η^2-*O*=C(Me)CH=*C*Ph) (**2**) and Cp*W(NO)(OEt)(η^2-*O*=C(Me)CH=*C*Ph) (**3**), respectively, in high yield and purity (eq 1). These four-legged, piano-stool complexes are burgundy crystalline solids that are air-stable at ambient temperatures for

$$\mathbf{1} \quad \xrightarrow[\text{- SiMe}_4 / 45\ °C]{\text{ROAc}} \quad \text{(structure)} \qquad (1)$$

2 R = Me
3 R = Et
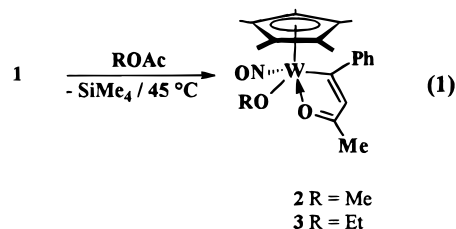
periods up to 1 week. The Nujol-mull IR bands attributable to the NO stretch in **2** and **3** are located at 1532 and 1538 cm^{-1}, typical of 18e alkoxide-containing complexes.[9] The ^{1}H and ^{13}C NMR signals displayed by complexes **2** and **3** are readily assigned. For example, the resonances of the acyl methyl substituents in the ^{1}H NMR spectra are singlets that integrate for 3 protons at about δ 2.32 and 2.44 for **2** and **3**, respectively, and the signals for the analogous carbon nuclei are identifiable in the ^{13}C NMR spectra at about 26 ppm for both complexes. Likewise, the vinyl proton resonance is evident as a singlet at 7.18 ppm for complex **2** and 7.37 ppm for complex **3**. The assignment of the carbon backbone containing the PhC=CH unit in these complexes is deduced from the combination of the gate-decoupled ^{13}C NMR results and from HMBC experiments. On the other hand, NOE and HMBC data do not distinguish between the structure depicted in eq 1 for **2** and **3** and the expected oxametallacyclopentene ring structure erroneously reported[8] to result from the simple reductive coupling of carbonyl and acetylene moieties in the metal's coordination sphere.

The four-legged piano-stool arrangement of ligands in the solid-state molecular structure of **2** has been definitively established by an X-ray crystallographic analysis (Figure 1). Of particular note is the existence of the tungsten-bound methoxy group (W−O bond length of 2.001(7) Å) that confirms a C−O bond-cleavage process, in addition to reductive coupling, affords the observed 18e products. The σ-bound methoxy and alkyl ligands are trans-disposed in the metal's coordination sphere, and the acyl function is coordinated in a cis fashion to both σ-ligands with a W−O dative bond length of 2.203(6) Å. Interestingly, this distance is shorter than the 2.535(7) Å Ni−O dative bond length in the late transition metal complex Ni(PMe$_3$)$_2$(Cl)(η^2-

(9) Legzdins, P.; Lundmark, P. J.; Rettig, S. J. *Organometallics* **1993**, *12*, 3545.

Table 3. ^{1}H and ^{13}C NMR Spectroscopic Data for Complexes 2, 4, 4-d_2, 8, 9, 11, and 11-d_6

compd no.	^{1}H NMR^a δ (ppm)	^{13}C NMR^a δ (ppm)
2	7.60 (d, 2H, $^3J_{HH}$ = 7.2 Hz, Ph o-H)	251.3 (O=CMe)
	7.37 (s, 1H, CPh=CH)	204.8 (CPh=CH)
	7.31 (vt, 2H, $^3J_{HH}$ = 7.2 Hz, Ph m-H)	150.1 (Ph i-C)
	7.31 (vt, 1H, $^3J_{HH}$ = 7.2 Hz, Ph p-H)	136.2 (CPh=CH)
	4.42 (s, 3H, MeO)	128.5 (Ph)
	2.44 (s, 3H, MeC=O)	127.9 (Ph)
	1.72 (s, 15H, C$_5$Me$_5$)	127.0 (Ph)
		112.7 (C_5Me$_5$)
		62.6 (OMe)
		26.3 (MeC=O)
		9.2 (C$_5$Me$_5$)
4	8.69 (br s, 1H, NH)	229.5 (s, CPh=CH)
	7.55 (d, 2H, $^3J_{HH}$ = 6.9 Hz, Ph o-H)	182.6 (s, HN=CMe)
	7.27 (vt, 2H, $^3J_{HH}$ = 7.2 Hz, Ph m-H)	150.9 (s, Ph i-C)
	7.18 (vt, 1H, $^3J_{HH}$ = 6.9 Hz, Ph p-H)	135.2 (d, $^1J_{CH}$ = 155.8 Hz, CPh=CH)
	7.06 (d, 1H, $^4J_{HH}$ = 3.5 Hz, CPh=CH)	127.8 (d, $^1J_{CH}$ = 156.7 Hz, Ph)
	2.25 (s, 3H, HN=CMe)	127.7 (d, $^1J_{CH}$ = 156.7 Hz, Ph)
	1.67 (s, 15H, C$_5$Me$_5$)	127.3 (d, $^1J_{CH}$ = 158.8 Hz, Ph)
	0.86 (br s, 1H, OH)	112.0 (s, C_5Me$_5$)
		23.6 (q, $^1J_{CH}$ = 132.0 Hz, HN=C(Me))
		9.7 (q, $^1J_{CH}$ = 127.4 Hz, C_5Me$_5$)
4-d_2	7.55 (d, 2H, $^3J_{HH}$ = 6.9 Hz, Ph o-H)	b
	7.27 (vt, 2H, $^3J_{HH}$ = 7.2 Hz, Ph m-H)	
	7.18 (vt, 1H, $^3J_{HH}$ = 6.9 Hz, Ph p-H)	
	7.06 (s, 1H, CPh=CH)	
	2.25 (s, 3H, ND=CMe)	
	1.67 (s, 15H, C$_5$Me$_5$)	
8	8.11 (br s, 1H, HN=CMe)	228.5 (s, CPh=CH)
	7.53 (d, 2H, $^3J_{HH}$ = 8.1 Hz, Ph o-H)	185.2 (s, HN=CMe)
	7.24 (vt, 2H, $^3J_{HH}$ = 8.1 Hz, Ph m-H)	175.9 (s, HN-C(=(C$_4$H$_4$))Me)
	7.24 (vt, 1H, $^3J_{HH}$ = 8.1 Hz, Ph p-H)	150.1 (s, Ph i-C)
	7.06 (d, 1H, $^4J_{HH}$ = 3.0 Hz, CPh=CH)	135.0 (d, $^1J_{CH}$ = 158.5 Hz, CPh=CH)
	6.52 (br s, 1H, HNC(=C(C$_4$H$_4$))Me)	127.9 (d, $^1J_{CH}$ = 159.2 Hz, Ph)
	6.50 (br s, 1H, HNC(=C(C$_2$H$_a$H$_b$C$_2$H$_2$))Me)	127.2 (d, $^1J_{CH}$ = 159.0 Hz, Ph)
	6.44 (br s, 1H, HNC(=C(C$_2$H$_a$H$_b$C$_2$H$_2$))Me)	127.1 (d, $^1J_{CH}$ = 159.0 Hz, Ph)
	6.23 (br s, 1H, HNC(=C(C$_2$H$_2$C$_2$H$_a$H$_b$))Me)	121.5 (br s, HNC=C(C$_4$H$_4$))Me)
	6.10 (br s, 1H, HNC(=C(C$_2$H$_2$C$_2$H$_a$H$_b$))Me)	117.8 (br s, HNC(=C(C$_4$H$_4$))Me)
	2.34 (s, 3H, HN=CMe)	115.6 (br s, HNC(=C(C_4H$_4$))Me)
	2.25 (s, 3H, HNC(=C(C$_4$H$_4$))Me)	115.0 (br, s, HNC(=C(C_4H$_4$))Me)
	1.70 (s, 15H, C$_5$Me$_5$)	111.7 (s, C_5Me$_5$)
		107.5 (br s, HNC(=C(C_4H$_4$))Me)
		23.7 (q, $^1J_{CH}$ = 127.9 Hz, N=CMe)
		21.2 (q, $^1J_{CH}$ = 128.3 Hz, HN−C(fulv)Me)
		9.7 (q, $^1J_{CH}$ = 128.0 Hz, C_5Me$_5$)
9	7.26 (d, 2H, $^3J_{HH}$ = 6.9 Hz, Ph o-H)	226.2 (s, CPh=CH)
	7.14 (t, 2H, $^3J_{HH}$ = 6.9 Hz, Ph m-H)	170.7 (s, N=CMe)
	7.08 (t, 1H, $^3J_{HH}$ = 6.9 Hz, Ph p-H)	150.3 (s, Ph i-C)
	6.59 (s, 1H, $^3J_{WH}$ = 14 Hz, CPh=CH)	134.5 (d, $^1J_{CH}$ = 157.5 Hz, CPh=CH)
	1.95 (s, 3H, HN=CMe)	127.5 (d, $^1J_{CH}$ = 158.0 Hz, Ph)
	1.51 (s, 15H, C$_5$Me$_5$)	126.8 (d, $^1J_{CH}$ = 158.0 Hz, Ph)
	1.35 (s, 3H, OCMe$_2$)	126.6 (d, $^1J_{CH}$ = 158.0 Hz, Ph)
	1.20 (s, 3H, OCMe$_2$)	113.0 (s, C_5Me$_5$)
		99.2 (s, (OCMe$_2$)
		30.1 (q, $^1J_{CH}$ = 127.5 Hz, OCMe_2)
		29.0 (q, $^1J_{CH}$ = 127.5 Hz, OCMe_2)
		18.3 (q, $^1J_{CH}$ = 127.5 Hz, HN=CMe)
		9.9 (q, $^1J_{CH}$ = 127.5 Hz, C_5Me$_5$)
11	7.43 (d, 2H, $^3J_{HH}$ = 8.1 Hz, Ph o-H)	191.8 (CPh=CH)
	7.26 (vt, 2H, $^3J_{HH}$ = 8.4 Hz, Ph m-H)	171.1 (NHC(Me)=N)
	7.11 (vt, 1H, $^3J_{HH}$ = 7.5 Hz, Ph p-H)	156.1 (NC=CH$_2$)
	6.83 (s, 1H, CPh=CH)	150.9 (Ph i-C)
	4.73 (br s, 1H, HNC(Me)=)	138.8 (d, $^1J_{CH}$ = 127.7 Hz, CPh=CH)
	4.45 (s, 1H, NC=CH_aH$_b$)	127.7 (Ph)
	4.28 (s, 1H, NC=CH$_a$H$_b$)	125.4 (Ph)
	2.11 (s, 3H, HNC(Me)=)	111.8 (C_5Me$_5$)
	1.73 (s, 15H, C$_5$Me$_5$)	90.6 (NC=CH$_2$, $^1J_{CH}$ = 152 Hz)
		22.8 (HNC(Me)=)
		9.9 (C$_5$Me$_5$)
11-d_6	7.43 (d, 2H, $^3J_{HH}$ = 8.1 Hz, Ph o-H)	b
	7.26 (vt, 2H, $^3J_{HH}$ = 8.4 Hz, Ph m-H)	
	7.11 (vt, 1H, $^3J_{HH}$ = 7.5 Hz, Ph p-H)	
	6.83 (s, 1H, CPh=CH)	
	2.11 (s, 3H, HNC(Me)=)	
	1.73 (s, 15H, C$_5$Me$_5$)	

^{a} Sample spectra recorded in CDCl$_3$ unless otherwise noted. ^{b} Spectrum not recorded.

Table 4. X-ray Crystallographic Data for Complexes 2, and 4, 8, and 10

	2	4	8	10
		Crystal Data		
empirical formula	$C_{21}H_{27}NO_3W$	$C_{22}H_{29}N_3O_2W$	$C_{31}H_{39}N_5OW$	$C_{25}H_{34}N_2O_2W$
cryst habit, color	long plate, red	prism, orange	irregular block, red	block, red
cryst size, mm	$0.32 \times 0.095 \times 0.012$	$0.50 \times 0.18 \times 0.18$	$0.28 \times 0.19 \times 0.08$	$0.28 \times 0.24 \times 0.19$
cryst syst	monoclinic	monoclinic	monoclinic	monoclinic
space group	$P2_1/c$	$P2_1/n$	$P2_1$	$P2_1/c$
vol, Å^3	1964.2(2)	2159.21(9)	1485.68(3)	2341.90(4)
a, Å	7.2421(3)	8.4729(2)	7.2125(1)	10.5087(1)
b, Å	15.3723(7)	21.2313(5)	18.4419(1)	15.4352(2)
c, Å	17.8615(8)	12.1060(3)	11.3542(2)	15.1367(1)
β, deg	98.962(1)	97.483(1)	100.348(1)	94.787(1)
z	4	4	2	4
fw	525.29	551.33	681.52	578.39
density (calcd, mg/m^3)	1.776	1.696	1.523	1.640
abs coeff, mm^{-1}	5.901	5.371	3.919	4.955
$F(000)$	1032	1088	684	1152
		Data Collection		
diffractometer	Siemens SMART Platform CCD	Siemens SMART Platform CCD	Siemens SMART Platform CCD	Siemens SMART Platform CCD
wavelength, Å	0.710 73	0.710 73	0.710 73	0.710 73
temp, K	173(2)	173(2)	173(2)	173(2)
θ range for data collection, deg	1.76−25.10	1.92−25.03	1.82−25.01	1.89−25.03
index ranges	$-8 < h < 8$, $-18 < k < 18$, $-20 < l < 21$	$-10 < h < 9$, $-25 < k < 25$, $-14 < l < 10$	$-8 < h < 8$, $-21 < k < 21$, $0 < l < 13$	$-11 < h < 11$, $0 < k < 18$, $0 < l < 17$
no. of reflns collected	9664	11 123	7150	11 298
no. of indep reflns	3457 ($R_{int} = 0.0522$)	3800 ($R_{int} = 0.0378$)	4957 ($R_{int} = 0.0199$)	4064 ($R_{int} = 0.0288$)
		Solution and Refinement		
system used	SHELXTL-V5.0	SHELXTL-V5.0	SHELXTL-V5.0	SHELXTL-V5.0
solution	direct methods	direct methods	direct methods	direct methods
refinement method	full-matrix least-squares on F^2	full-matrix least-squares on F^2	full-matrix least-squares on F^2	full-matrix least-squares on F^2
weighting scheme	$w = 2(F_o^2) + (AP)^2 + (BP)]^{-1}$, where $P = (F_o^2 + 2F_c^2)/3$, $A = 0.0546$, and $B = 0.0$	$w = 2(F_o^2) + (AP)^2 + (BP)]^{-1}$, where $P = (F_o^2 + 2F_c^2))/3$, $A = 0.0139$, and $B = 3.9846$	$w = 2(F_o^2) + (AP)^2 + (BP)]^{-1}$, where $P = (F_o^2 + 2F_c^2)/3$, $A = 0.0384$, and $B = 0.789$	$w = 2(F_o^2) + (AP)^2 + (BP)]^{-1}$, where $P = (F_o^2 + 2F_c^2))/3$, $A = 0.0136$, and $B = 1.1696$
abs corr	SADABS (Sheldrick, 1996)	semiempirical	SADABS (Sheldrick, 1996)	SADABS (Sheldrick, 1996)
max and min transmission	1.000 and 0.572	0.66286 and 0.39415	1 and 0.835	1 and 0.784
data/restraints/params	3455/0/243	3800/0/288	4955/1/343	4064/0/280
final R indices [$I > 2\sigma(I)$]	$R_1 = 0.0516$, $wR_2 = 0.1031$	$R_1 = 0.0223$, $wR_2 = 0.0489$	$R_1 = 0.0284$, $wR_2 = 0.0675$	$R_1 = 0.0277$, $wR_2 = 0.0479$
R indices (all data)	$R_1 = 0.0791$, $wR_2 = 0.1117$	$R_1 = 0.0271$, $wR_2 = 0.0512$	$R_1 = 0.0326$, $wR_2 = 0.0697$	$R_1 = 0.0401$, $wR_2 = 0.0506$
goodness-of-fit on F^2	1.059	1.125	1.04	1.072
largest diff. peak and hole, e Å^{-3}	1.794 and −2.329	0.576 and −0.730	0.616 and −0.729	0.452 and −0.542
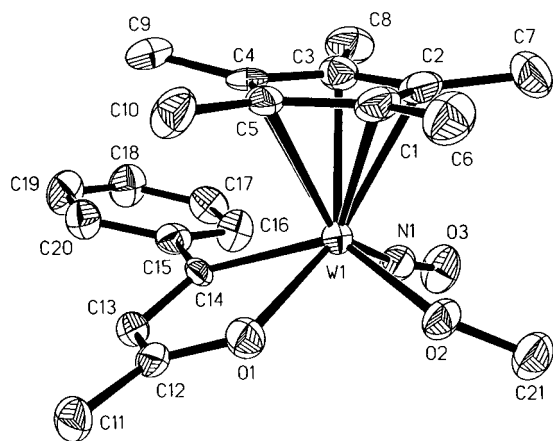
Figure 1. Thermal ellipsoid plot of compound **2**. Thermal ellipsoids depict the 50% probability level.

Scheme 3
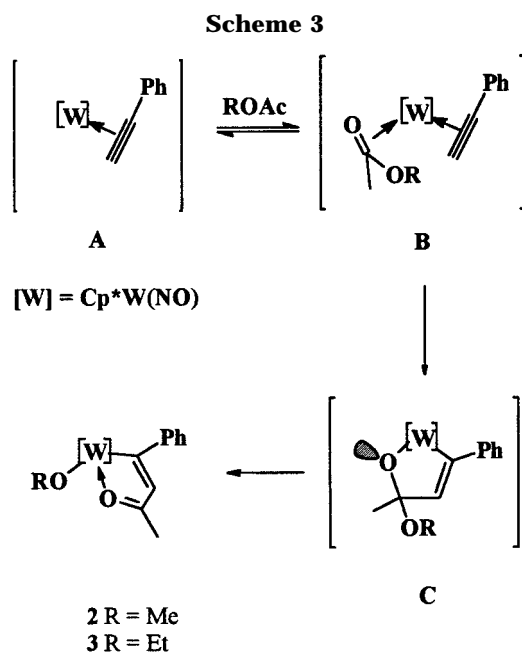
O=C(CH$_2$SiMe$_3$)C=CPh)[10] as well as the 2.361(3) Å Zr−O bond length previously reported by Rosenthal for related zirconacyclic complexes[11] yet longer than the Re−O bond length of 2.099 Å in the isoelectronic [CpRe-(NO)(PPh$_3$)(η^1-O=CMePh)]$^+$ cation.[12] The C=O bond length of 1.277(12) Å is longer than a typical C−O double bond and is characteristic of a coordinated acyl function.[13] The oxametallacyclopentadiene ring is clearly evident from the short−long−short pattern of bond lengths for the O(1)=C(12)−C(13)=C(14) fragment (1.277(12), 1.413(14), and 1.337(12) Å, respectively), comparable to those found in the structure of the above-mentioned Ni (II) complex.

The mechanism that we propose for the overall process leading to **2** and **3** is depicted in Scheme 3. Intermediate **B**, formed by coordination of an ester to W in **A**, is transformed into the oxametallacyclopentene

Scheme 4
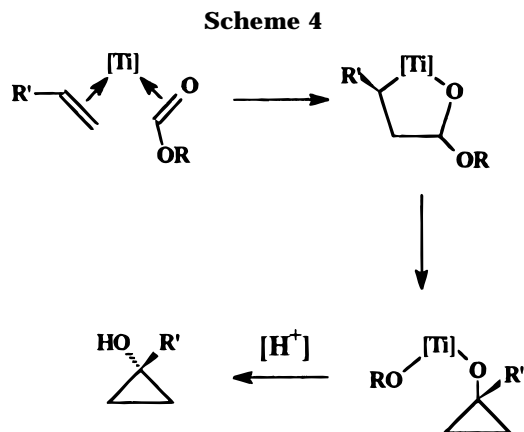
C by the reductive coupling of the two coordinated ligands. While the analogous Cp$_2$Zr oxametallacyclopentene complexes are readily isolable and have been studied extensively,[3b,d] the Cp*W(NO)-containing intermediate **C** cannot be isolated as such. Indeed, though the metal-bound acetal O has the capacity to function as a 3e donor to the metal center in the correct orientation[14] and as such would render the complex electronically saturated, space-filling models reveal that the restrictive geometry of the five-membered ring enforces a conformation that leaves the filled O-centered orbitals pointed away from the metal center. The O atom, thus, functions predominantly as a 1e donor, resulting in a build-up of electron density at the heteroatom and leaving the metal center in **C** electronically unsaturated. Subsequent acetal C−O-bond cleavage yields the observed 18e complexes.

Only one of two possible routes to the observed products is presented in Scheme 3. An alternate path involving direct acyl C−O oxidative addition to the metal center in **A** followed by acyl/acetylene coupling is conceivable, yet such examples involving alkyl carboxylate esters are rare and reports of this mode of reactivity seem limited to low-valent late transition metal systems.[15] On the other hand, coordination of an ester is a prerequisite to reductive coupling, and our recent observation of η^2-ester coordination in the related Cp*W(NO)(PPh$_3$) fragment[16] supports a pathway involving the intermediacy of B.

Acetal β-C−O bond cleavage by a TM complex is an area of considerable current interest, probably the most well-known example being the Kulinkovich reaction which generates cyclopropanols following reductive coupling of the coordinated olefin and ester at Ti(II) centers (Scheme 4).[17] While the coupling leading to complexes **2** and **3** is reminiscent of the Kulinkovich reaction, the products of the two reactions are quite different. Displacement of RO$^-$ in the putative acetal intermediate **C** by nucleophilic attack of the quaternary vinyl C at the acetal carbon center to give the O-bound

(10) Carmona, E.; Gutiérrez-Puebla, E.; Monge, A.; Marín, J. M.; Paneque, M.; Poveda, M. *Organometallics* **1989**, *8*, 967.

(11) Peulecke, N.; Ohff, A.; Tillack, A.; Baumann, W.; Kempe, R.; Burlakov, V. V.; Rosenthal, U. *Organometallics* **1996**, *15*, 1340.

(12) Dalton, D. M.; Fernández, J. M.; Emerson, K.; Larsen, R. D.; Arif, A. M.; Gladysz, J. A. *J. Am. Chem. Soc.* **1990**, *112*, 9198.

(13) Debad, J. D.; Legzdins, P. *Organometallics* **1993**, *12*, 2094.

(14) (a) Ashby, M. T.; Enemark, J. H. *J. Am. Chem. Soc.* **1986**, *108*, 730. (b) Hubbard, J. L.; McVicar, W. K. *Inorg. Chem.* **1992**, *31*, 910.

(15) For a review of this chemistry, see: Yamamoto, A. *Adv. Organomet. Chem.* **1992**, *34*, 111.
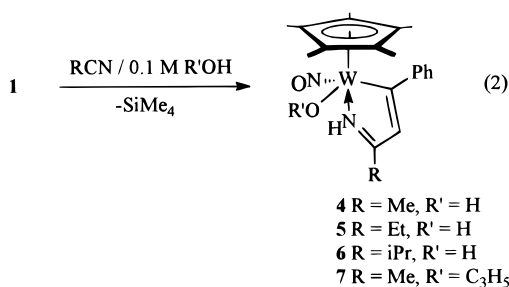
(16) Burkey, D. J.; Debad, J. D.; Legzdins, P. *J. Am. Chem. Soc.* **1997**, *119*, 1139.

(17) (a) Lee, J.; Kim, H.; Cha, J. K. *J. Am. Chem. Soc.* **1996**, *118*, 4198. (b) Lee, J.; Kim, H.; Cha, J. K. *J. Am. Chem. Soc.* **1996**, *118*, 291. (c) Corey, E. J.; Rao, A. R.; Noe, M. C. *J. Am. Chem. Soc.* **1994**, *116*, 9345. (d) Kulinkovich, O. G.; Sviridov, S. V.; Vasilevskii, D. A. *Synthesis* **1991**, *3*, 234.

cyclopropenyl ligand (as proposed to account for the products in the Kulinkovich reaction) is not observed, presumably a result of the reduced oxophilicity of W(II) relative to Ti(IV) and the greater ring strain in cyclopropene relative to cyclopropane.[18] Other examples of acetal β-C−O bond cleavage have been described in the literature. Yamamoto has reported the generation of acetal complexes by the addition of a M−H bond (M = Rh,[19a] Co[19b]) across the carbonyl function of the coordinated ester and subsequent β-C−O bond cleavage to produce the analogous aldehydes. Likewise, Grotjahn has recently invoked acetal C−O bond cleavage to account for the thermal generation of an alkoxycarbene complex from a CpRu acetal complex.[20] Given these literature precedents, the pathway outlined in Scheme 3 appears to be the more reasonable one. While numerous examples of an ester coupling to an olefin exist, the reductive coupling of an ester to an acetylene in the coordination sphere of a metal appears to be unprecedented. Because the overall transformation involves the formal exchange of vinyl for alkoxide at the acyl carbon, this reaction can be viewed as the conversion of a carboxylate ester to an α,β-unsaturated ketone via C−O bond cleavage.[21] Variation of the ester substituents and the precursor vinyl substituents, thus, offers potential access to a range of substituted vinyl ketones.

Reductive Coupling with Nitriles. Simple reductive coupling of acetylene and coordinated nitrile in the tungsten's coordination sphere does not yield the expected azametallacycle, Cp*W(NO)(η^2-N=C(R)CH=CPh), following the generation of the acetylene intermediate **A** in nitrile solvent. Instead, analogous to the thermolysis of **1** in esters, the products obtained result from the subsequent reactivity of the intermediate azametallacyclopentadiene complex obtained through initial reductive coupling. Unlike the acetal intermediate **C**, however, this aza complex does not achieve electronic saturation by rearrangement. Rather, trapping of this intermediate by a variety of electrophilic sources occurs.

A. Trapping by Protic Sources. Thermolysis of **1** in nitrile-containing 0.1−0.01 M H$_2$O or allyl alcohol affords complexes **4−7** quantitatively (eq 2). These

$$1 \xrightarrow[\text{−SiMe}_4]{\text{RCN / 0.1 M R'OH}} \quad (2)$$

4 R = Me, R' = H
5 R = Et, R' = H
6 R = iPr, R' = H
7 R = Me, R' = C$_3$H$_5$

products are orange-red crystalline solids that are air-

Figure 2. Thermal ellipsoid plot of complex **4**. Thermal ellipsoids depict the 50% probability level.

stable for periods of up to 2 weeks at ambient temperatures, thereby attesting to the existence of an 18e, closed-shell configuration at the metal center. The solid-state molecular structure of prototypal complex **4** is shown in Figure 2. Analogous to the structure of complex **2**, imine N coordination to W diagonal to the NO ligand in these four-legged piano-stool complexes confers electronic saturation at the metal center. Although the hydroxyl H was not located during the structure refinement, the W−O bond length of 2.064(2) Å is characteristic of a tungsten−oxygen single bond.[22] Hence, protonation at the coordinated imine must be invoked to support the hybridization at N and to preserve the electroneutrality of the complex.

The solid-state structural features highlighted in the preceding paragraph are also evident in the spectroscopic data for complex **4** (Table 3). For example, signals for both the N−H and O−H protons are visible in the ^{1}H NMR spectra (CDCl$_3$) of complexes **4−6**, the former appearing at approximately 8.65 ± 1.0 ppm and the latter in the range 0.84 ± 0.2 ppm. In addition, the singlet attributable to the vinyl H in all cases appears at about 7.1 ppm ($^1J_{CH} \approx 157$ Hz). Signals in the ^{13}C-{^{1}H} NMR spectrum at about 228 and 189 ± 7 ppm divulge the presence of the carbenoid C$_\alpha$ atom of the vinyl moiety and the quaternary imine carbon, respectively. The downfield shift of the resonance due to the carbenoid C$_\alpha$ atom suggests a degree of electronic delocalization in the azametallacyclopentadienyl ring.[23]

Interestingly, only the O−H stretch in the Nujol-mull IR spectrum of **4** is readily observable, the N−H stretch being masked by the broad unsaturated C−H absorptions in the range 3000−3200 cm^{-1} (Table 2). However, the isotopic shift of these absorptions in the IR spectrum can be examined for the complex in which a deuterium label is incorporated at the hydroxyl and imido sites (eq 3). The Nujol-mull IR spectrum of **4**-d_2 reveals a band at 2282 cm^{-1} which can be attributed to the N−D stretch. Calculation of the expected N−H stretch for complex **4** based on the Redlich−Teller rule[24] gives a value of ν_{N-H} for **4** of 3195 cm^{-1}, in a region obscured

(18) A recent theoretical analysis describes ring strain and bond enthalpies as the major contributors to the stability of methylcyclopropane relative to methylcyclopropene, see: Johnson, W. T. G.; Borden, W. T. *J. Am. Chem. Soc.* **1997**, *119*, 5930.

(19) (a) Yamamoto, T.; Miyashita, S.; Naito, Y.; Komiya, S.; Ito, T.; Yamamoto, A. *Organometallics* **1982**, *1*, 808. (b) Hayashi, Y.; Yamamoto, T.; Yamamoto, A.; Komiya, S.; Ito T.; Kushi, Y. *J. Am. Chem. Soc.* **1986**, *108*, 385.

(20) Grotjahn, D. B.; Lo, H. C. *Organometallics* **1996**, *15*, 2860.

(21) For other examples of ketone-stabilized vinyl complexes, see: (a) Alt, H. G.; Eichner, M. E.; Jansen, B. M. *Angew. Chem., Int. Ed. Engl.* **1982**, *21*, 861. (b) Alt, H. G.; Hayen, H. I. *J. Organomet. Chem.* **1986**, *103*, 1501. (c) Bianchini, C.; Innocenti, P.; Melli, A.; Sabat, M. *Organometallics* **1986**, *5*, 72. (d) Reference 10.
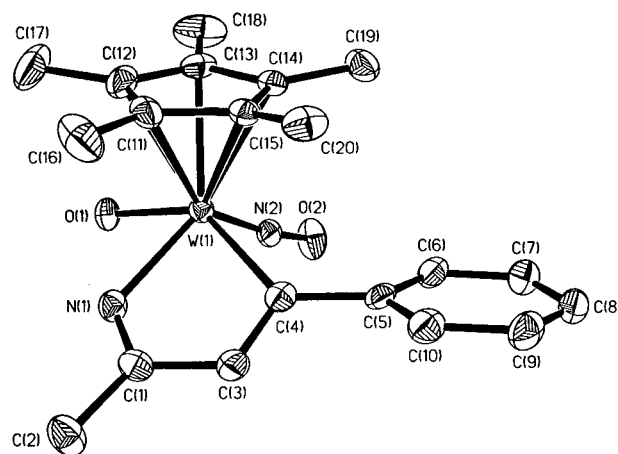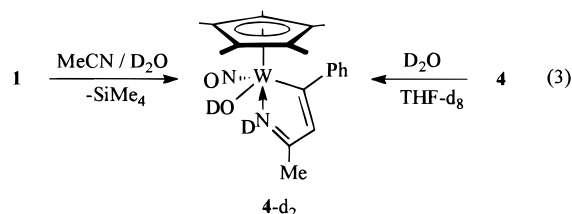
(22) The complex [Mo(O)(OH)(CN)$_4$]$^{3-}$ has Mo=O = 1.697(7) Å and Mo−OH = 2.077(7) Å; see: Robinson, P. R.; Schlemper, E. O.; Murmann, R. K. *Inorg. Chem.* **1975**, *14*, 2035. Typical terminal W−oxo bond distances lie in the range 1.68−1.72 Å, see: Nugent, W. A.; Mayer, J. M. *Metal Ligand Multiple Bonds*; Wiley: New York, 1988.

$$1 \xrightarrow[-SiMe_4]{MeCN / D_2O} \quad \mathbf{4\text{-}d_2} \quad \xleftarrow[THF\text{-}d_8]{D_2O} \quad 4 \quad (3)$$

by the bands resulting from the vinylic and aromatic C−H stretches. Prediction of the O−D stretch expected for **4**-d_2 employing the same calculation based on the observed ν_{O-H} for **4** yields a value of 2544 cm^{-1}, which is in reasonable agreement with the experimentally observed value of 2630 cm^{-1}.

Other protic sources with pK_a values comparable to that of water can also be employed as trapping reagents in this reaction. For example, thermolysis of **1** in acetonitrile containing small amounts of allyl alcohol results in the formation of the alkoxide complex **7**, which can be isolated in good yield as air-stable red crystals. The N−H proton resonance in the ^{1}H NMR spectrum of allyl **7** is a singlet at 8.62 ppm, analogous to that exhibited by the hydroxyl complex **4**. Signals attributable to the allylic moiety of the alkoxide ligand are distinguishable as a series of multiplets in the characteristic range of δ 4.5−6.2.[25] The remaining spectroscopic data are consistent with the formulated structure and are readily assigned by comparison to the data for complexes **4**−**6**.

The proposed mechanism to account for this reactivity is shown in Scheme 5. Following the initial generation of **A**, coordination of RC≡N (R = Me, Et, ^{i}Pr) and reductive coupling of acetylene and nitrile in the metal's coordination sphere give the azametallacyclopentadienyl intermediate **E**. The geometry of the resulting five-membered ring enforces an imide conformation that severely restricts the donation of the nitrogen atom's sp^2 lone-pair electron density to the metal. Hence, the imide N only functions as a 1e donor, and the result is a 16e, Lewis acidic complex. Analogous to intermediate **C**, the build-up of lone pair electron density on the imido N in **E** renders it susceptible to protonation by the external protic source, R′OH. The hydration of **E** and coordination of the amido N in a manner analogous to the acyl O in **C** thus affords the observed 18e products. Similar protonated or alkylated azametallacyclopentadienyl complexes of Ti,[26a] Nb,[26b] Ta,[26c] W[26d,e] and Ir[26f] have been synthesized via analogous or other preparative routes.

Mechanistic studies have afforded evidence in support of the reaction pathway proposed in Scheme 4. Incorporation of deuterium at the amine and hydroxyl

Scheme 5
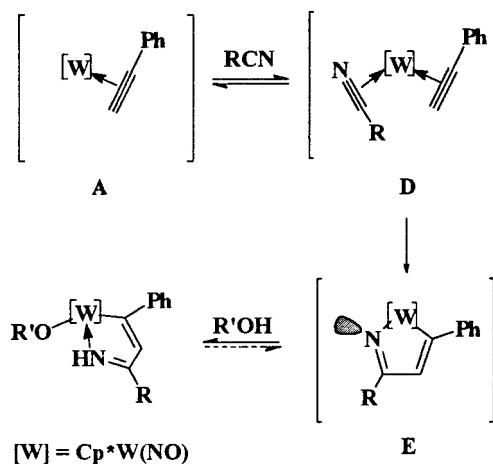
positions occurs during the thermolysis of hydroxide **4** in THF-d_8 containing D$_2$O (vide supra), thereby implying that these two protons are labile. In addition, the thermolysis of allyl **7** in wet THF-d_8 results in its conversion to complex **4**, at a rate significantly slower than that observed for label exchange. Taken together, these results indicate that the two processes are independent. In other words, while the hydroxyl and amine protons are labile and readily exchange in the presence of D$_2$O, the formation of alkoxide complexes **4**−**7** by the addition of R′OH is slow by comparison, with interconversion probably being governed by the pK_a of the two protic sources.[27] Because **E** is a high-energy intermediate, it is uncertain whether the hydration step can be regarded as reversible. On the other hand, the formation of a strong C−C single bond and the conjugation within the ligand backbone strongly suggests that the **D** → **E** ring closure is irreversible. It is also pertinent that the analogous thermolysis in wet ^{t}BuCN does not afford any tractable products. While an η^1 interaction of the bulkier ^{t}BuCN with the metal center can presumably occur, unfavorable steric interactions probably slow either the formation of intermediate **D** or the **D** → **E** ring-closing step to the extent that decomposition pathways, thus, become competitive and no product is observed. Interestingly, the coupling of two ^{t}BuC≡CH units on the (RO)$_3$Ta fragment (RO = 2,6-diisopropylphenoxide) reported by Wigley is facile at room temperature.[28] Even more striking is the fact that under thermolysis conditions, ^{t}BuCN couples readily to coordinated benzyne in the Buchwald Cp$_2$Zr system.[29] It would, thus, appear that the substantial size of the Cp* and phenyl acetylene ligands in our complexes is playing a significant role in the chemo- and regioselectivity leading to complexes **4**−**7**.

In light of the mechanism invoked to account for the formation of complexes **4**−**7** (vide supra), next we chose cyclopentadiene (CpH) as an atypical protic source to probe the extent of this reactivity. In doing so we discovered the unexpected result that under these

(23) Aromaticity has been invoked for similar aza- and thiapentadienyl iridium systems, see: (a) Alvarado, Y.; Daff, P. J.; Pérez, P. J.; Poveda, M. L.; Sánchez-Delgado, R.; Carmona, E. *Organometallics* **1996**, *15*, 2192. (b) Bleeke, J. R.; Ontwerth, M. F.; Rohde, A. M. *Organometallics* **1995**, *14*, 2813.
(24) Ebsworth, E. A. V.; Rankin, D. W. H.; Cradock, S. *Structural Methods in Inorganic Chemistry*; Blackwell Scientific Publications: London, 1987; pp 217−218.
(25) Debad, J. D.; Legzdins, P.; Lumb, S. A. *Organometallics* **1995**, *14*, 2543.
(26) (a) Cohen, S. A.; Bercaw, J. E. *Organometallics* **1985**, *4*, 1006. (b) Lorente, P.; Carfagna, C.; Etienne, M.; Donnadieu, B. *Organometallics* **1996**, *15*, 1090. (c) Strickler, J. R.; Wigley, D. E. *Organometallics* **1990**, *9*, 1665. (d) Filippou, A. C.; Völkl, C.; Kiprof, P. *J. Organomet. Chem.* **1991**, *415*, 375. (e) Filippou, A. C.; Völkl, C.; Rogers, R. D. *J. Organomet. Chem.* **1993**, *463*, 135. (f) Reference 23a.

(27) Lowry, T. H.; Richardson, K. S. *Mechanism and Theory in Organic Chemistry*, 2nd ed.; Harper & Row: New York, 1981.
(28) Smith, D. P.; Strickler, J. R.; Gray, S. D.; Bruck, M. A.; Holmes, R. S.; Wigley, D. W. *Organometallics* **1992**, *11*, 1275.
(29) Buchwald, S. L.; Watson, B. T.; Lum, R. T.; Nugent, W. A. *J. Am. Chem. Soc.* **1987**, *109*, 7137.
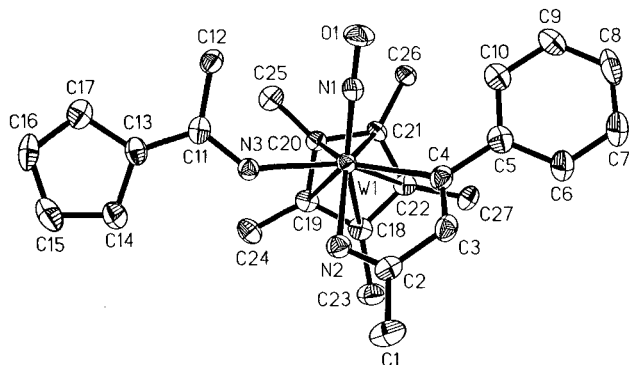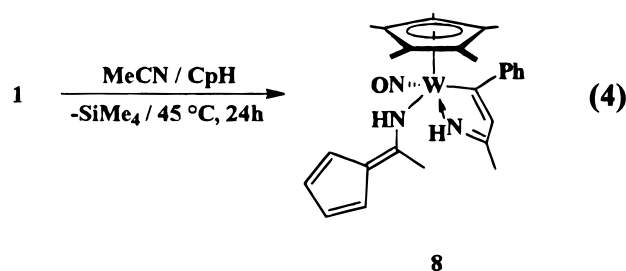
Figure 3. Thermal ellipsoid plot of compound **8**. Thermal ellipsoids depict the 50% probability level.

experimental conditions a second molecule of aceto-nitrile is incorporated into the complex and a fulvene substituent is obtained from the cyclopentadienyl fragment (eq 4). Solution ^{1}H NMR data (CDCl$_3$) for this

red-brown crystalline product are consistent with the existence of the protonated azametallacyclopentadienyl ring found in the molecular structures of complexes **4–7**. The results of a single-crystal X-ray diffraction study confirm the structure shown for fulvene complex **8** in eq 4.

The solid-state molecular structure depicted in Figure 3 reveals that the second molecule of MeCN is incorporated into the complex as a component of an aminopentafulvene ligand. In addition, the angles around both C(11) and C(13) sum to 360.0°, in accord with the proposed sp^2 hybridization at these centers, revealing the fulvene character in this five-membered ring. On the other hand, the C(11)–C(13) bond length and the fulvene ring bond lengths in 8 deviate substantially from those in the analogous 6,6-dimethylpentafulvene,[30] the C(sp^2)=C(sp^2) bonds containing significant single-bond character and the single bonds being contracted relative to the accepted C(sp^2)-C(sp^2) bond length. A structural study of the influence of dipolar resonance forms in aminopentafulvenes conducted by Ammon has revealed that the presence of the electron-releasing amine substituent results in significant charge separation in the ground state of the molecule; i.e., resonance structures **a** and **b** depicted in Figure 4 make a significant contribution to the ground state.[31]

The aminopentafulvene N in **8** functions as a 1e donor as a result of the electronic saturation of the metal center. Thus, it reasonable to assume that a substantial contribution by resonance form **b** to the ground state of the aminopentafulvene ligand is being reflected in the structural parameters determined for this ligand.
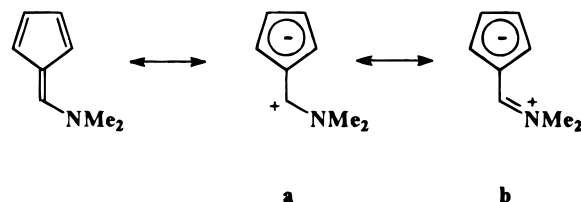
(30) Chiang, J. F.; Bauer, S. H. *J. Am. Chem. Soc.* **1970**, *92*, 261.

Figure 4. Resonance contributors to the electronic structure of dimethylaminopentafulvene.

Examination of the solution behavior of **8** by ^{1}H NMR spectroscopy reveals the intriguing fluxional nature of the aminofulvene ligand, further evidence for the electronic influence of the amine group (and resonance form **b**, Figure 4) on the structure of the fulvene ring (vide supra). The four fulvene H resonances in the ^{1}H NMR spectrum (CDCl$_3$) appear in the region δ 6.5–6.1. The broadness of these signals and the lack of observed interproton coupling in the RT (room temperature) spectrum are both symptomatic of a fluxional process. Consistently, changing the NMR solvent to toluene-d_8 results in a shift of the fulvene signals into the aromatic region and their coalescence into two broad singlets, implying a fluxional process that is faster in the less-polar solvent. Indeed, a VT-^{1}H NMR experiment (MeCN-d_3) reveals that at 60 °C the α- and α'-H signals coalesce to a broad singlet, as do the β- and β'-H signals. No further change occurs with an increase in temperature. Because the four sites are inequivalent in the static fulvene unit, coalescence implies that the α-site is equilibrating with the α'-site, as is the β- with the β'-site, through a rotation about the fulvene C_2 axis (Scheme 6, A). The approximate rotation rate of 272(5) s^{-1} at coalescence corresponds[32] to a $\Delta G^{\ddagger} =$ 15.3(2) kcal mol^{-1}. The source of this hindered rotation presumably lies in the partial reduction of the unique C=C bond order, as highlighted in the structural discussion above. Although a double bond is drawn between the two unique carbon nuclei of the fulvene unit in the formal bonding depiction, delocalization of amine lone-pair electron density to the N–C bond imparts considerable single-bond character to the fulvene linkage, permitting hindered rotation about this axis.

In addition, the ^{1}H NMR spectrum of **8** in CDCl$_3$ containing added D$_2$O shows the surprising result that ^{2}H label is incorporated into the α- *and* α'-H positions (δ 6.50 and 6.44 in the ^{1}H NMR spectrum) but *not* into either of the β-H positions, in addition to the expected exchange at the two amine sites. Consistently, selective irradiation of the fulvene amine H signal results in a dramatic reduction in intensity of both α-H signals by equivalent amounts via magnetization transfer between the amine-H and two α-H sites. An exchange process is, thus, implicated (Scheme 6, B). A 1,4-H shift transfers H$_n$ to the α-position, yielding two equivalent α-H bound to the sp^3 α-C. In the microscopic reverse, either one of these two protons may be transferred back to the amine N. Since the amine N readily exchanges with D$_2$O, label is incorporated into the fulvene ring via mechanism B. Because the label appears in *both* the α and α' sites in the slow-exchange RT spectrum, the exchange mechanism (B) must be operating indepen-

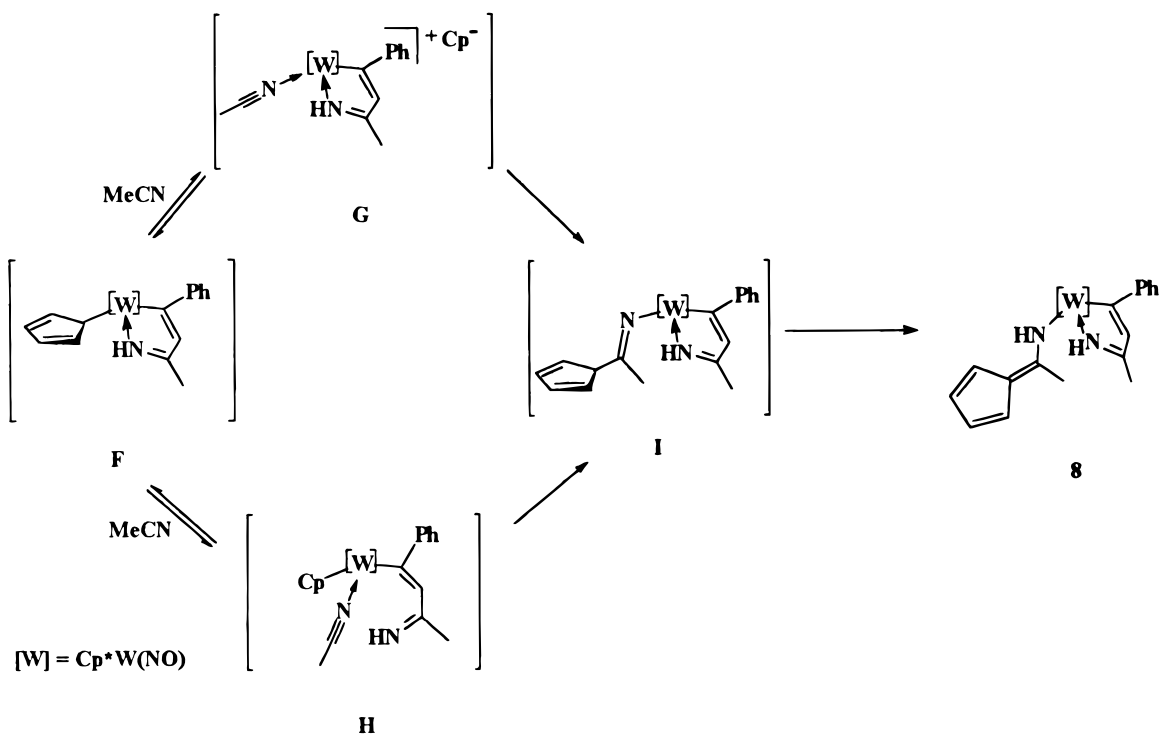(31) Ammon, H. L. *Acta Crystallogr., Sect. B* **1974**, *30*, 1731.
(32) Günther, H. *NMR Spectroscopy;* Wiley: New York, 1980.

Scheme 6

$[W] = Cp*W(NO)(\eta^2\text{-}HN=C(Me)CH=CPh)$

Scheme 7

$[W] = Cp*W(NO)$
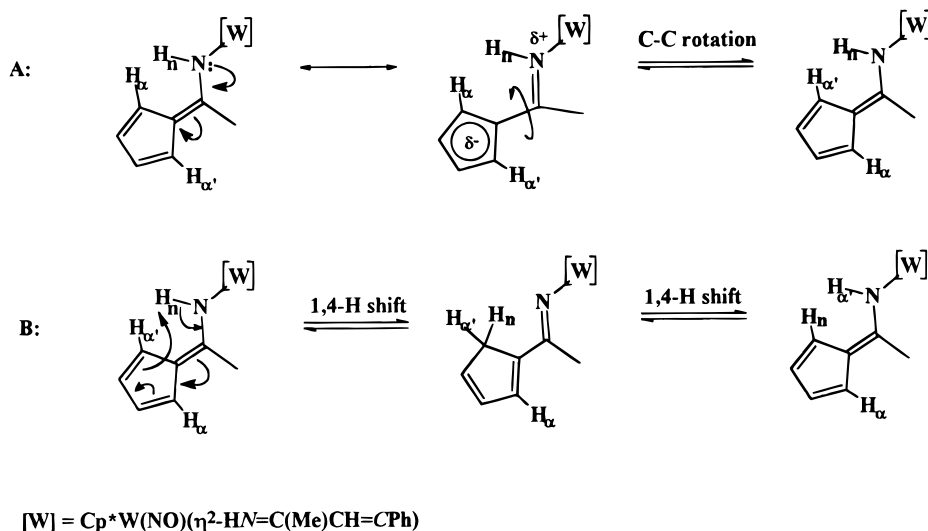
dent of the rotational mechanism (A) to corroborate the experimental observations.[33] That this process is significantly slower than fulvene rotation is established by the simultaneous reduction of the H_α and $H_{\alpha'}$ signal intensity upon irradiation of H_n. Unfortunately, the separate measurement of the H_n exchange rate at coalescence by magnetization transfer NMR spectroscopy is hampered by the near-coincidence of the coalescent H_α signals and that of H_n.

The mechanism to account for the formation of **8** is shown in Scheme 7 and is most easily expressed as a continuation of that presented in Scheme 4 for complexes **4**−**7**. Protonation by CpH at the basic imido site in **E** affords **F**, an intermediate analogous to compounds

4−**7**. Acetonitrile insertion may then proceed via one of two pathways. Dissociation of either Cp^- or the pendent imine followed by MeCN coordination yields the adducts **G** or **H**, respectively. Attack at the quaternary nitrile carbon by Cp^- in an inter- or intramolecular fashion then affords the azomethine intermediate **I**, and a 1,3-H tautomerization yields the observed enamine product.

Either pathway leading to **I** is plausible. The pendent imine fragment certainly could possess a degree of lability under the thermolysis conditions employed. Likewise, outer-sphere "η^0" Cp^- anions have been reported, but these seem to predominate in conjunction with late transition metal coordination compounds.[34] Considerable literature precedent exists for the η^1-

(33) An *intermolecular* exchange cannot be absolutely discounted, but the kinetic inaccessibility of the fulvene α-H suggests that such a process is unlikely.

(34) Casey, C. P.; O'Connor, J. M.; Haller, K. J. *J. Am. Chem. Soc.* **1985**, *107*, 1241.

bonding mode of the Cp ligand,[35] although examples of insertion chemistry into such metal−carbon linkages are scarce. Casey has described the formation of an oxafulvene of rhenium by the insertion of CO into a Re−η^1-Cp bond in the presence of PMe$_3$.[34] More recently, Carmona has reported the formation of the C-bound aminofulvene ligand [C(=C(C$_4$H$_4$))N(H)^{t}Bu] by invoking a 1,3-H shift in the imido ligand derived from the insertion of ^{t}BuNC into the Pd−C bond of an η^1-Cp ligand.[36]

B. Addition of the Carbonyl Function across the W−N Bond. We have suggested that the chemistry occurring beyond the initial reductive coupling event leading to compounds **2**−**8** results because the hetero-atom lone pair does not stabilize the 16e W center in intermediates **C** and **E** (vide supra). The nature of products **4**−**8** derived from the thermolyses in nitrile solvents containing protic acids and the proposed pathway by which they form reflect both the nucleophilic character of the imido nitrogen atom conferred by a build-up of electron density at N and the resultant electronic unsaturation of the metal center in **E**.

Further evidence supporting this rationale is provided by the very interesting and unusual products derived from the thermolysis of **1** in 0.1 M solutions of acetone in MeCN or ^{i}PrCN. After 24 h at 45 °C in these solutions, the alkyl vinyl complex **1** is cleanly converted to **9** or **10**, respectively (eq 5). These product complexes

$$\text{1} \xrightarrow[\text{−SiMe}_4 \,/\, 45\,°C, 24\,h]{\text{RCN / 0.1M acetone}} \quad (5)$$

9 R = Me
10 R = iPr
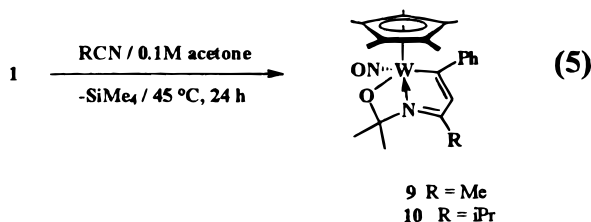
are isolable in relatively high yields from their respective reaction mixtures as red-brown crystalline blocks and are air-stable in the solid state for up to 2 weeks. Analogous to complexes **4**−**8** described previously, the phenyl ring, vinyl proton, and methyl substituent are readily identified from the characteristic signals in the ^{1}H and ^{13}C NMR spectra of **9** in CDCl$_3$ (Table 3). While these assignments are straightforward, extra signals in the proton and carbon spectra exist which are in accord with the presence of two additional methyl substituents and an extra quaternary carbon nucleus. The masses of the parent ions in the mass spectra of **9** and **10** are consistent with the inclusion of one molecule of acetone in the molecular formulas for these complexes, a feature also corroborated by their elemental analyses.

That acetone is incorporated into these extended ring systems is unequivocably confirmed by the solid-state molecular structure detemined for complex **10** by X-ray crystallography (Figure 5). The carbonyl unit has clearly added across the W−N bond yielding a C(11)−N(2) single bond distance of 1.478(5) Å and a W(1)−O(1) single bond length of 2.075(3) Å. Likewise, the C(11)−O(1) distance of 1.425(5) Å reflects the reduction of the C−O bond order to that of a single bond. The sum of the bond angles about N(2) (360.0°) reveals the sp^2 nature of the imine moiety, and the W(1)−N(2)
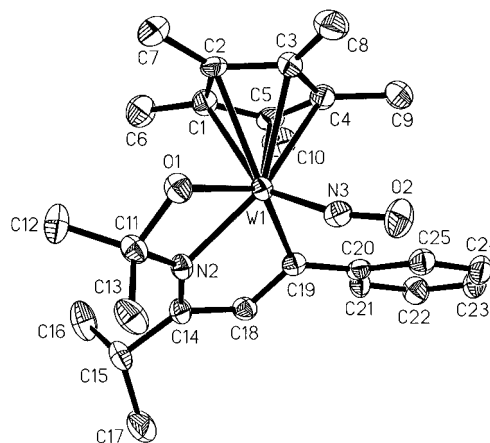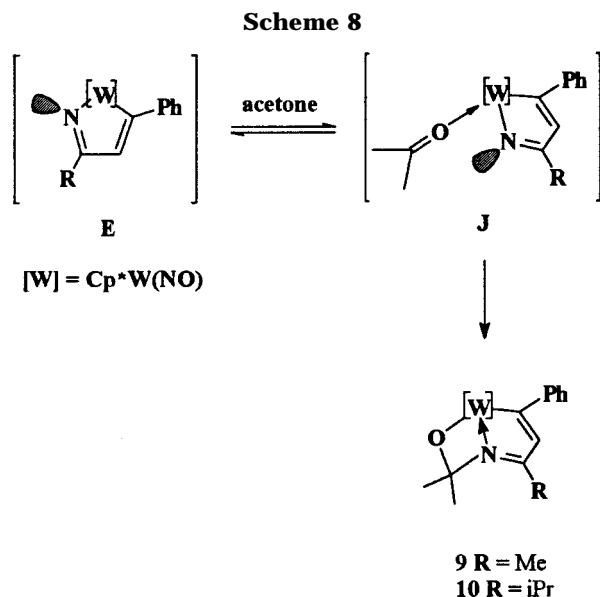
(35) O'Connor, J. M.; Casey, C. P. *Chem. Rev.* **1987**, *87*, 307.

Figure 5. Thermal ellipsoid plot of complex **10**. Thermal ellipsoids depict the 50% probability level.

Scheme 8

[W] = Cp*W(NO)

9 R = Me
10 R = iPr

distance of 2.095(3) Å is characteristic of coordination of N to W.[25]

The mechanism we propose to yield complexes **9** and **10** is depicted in Scheme 8 and, like that proposed for **8**, stems from the generation of the 16e intermediate **E** containing a nucleophilic imido N center. Following the formation of **E**, acetone coordination (**J**) facilitates the addition of the W−N bond across the carbonyl fragment. The regioselectivity of this addition reflects both the affinity of W for O[1a] as well as the polarity of the W−N linkage; the nucleophilic imido N attacks at the electrophilic quaternary carbonyl carbon with concomitant O attack at the electrophilic, electronically unsaturated metal center. That **9** and **10** are formed exclusively implies that the **J** → product step is irreversible. Consistently, **9** does not convert to **4** under thermolysis conditions in wet THF-d_8. At present, this ring expansion seems to be limited to sterically unencumbered ketones and aldehydes. For example, an NMR-scale thermolysis of **1** in MeCN containing small amounts of acetaldehyde affords the analogous addition products, as evinced in the ^{1}H NMR spectrum (CDCl$_3$) of the final reaction mixture. Two signals of equal intensity are observed for each environment, thereby implying the formation of two regioisomers in which the methyl substituent of the alkoxy fragment is presumably

directed either toward or away from the Cp* ring. In contrast, the analogous thermolyses in acetonitrile solvent containing small amounts of larger substrates such as ethyl acetate, dimethyl acetamide, or benzaldehyde afford only complex **11** (vide infra) and small amounts of unidentified decomposition products. An interesting observation is the selectivity of intermediates **A** and **E** for the reagents in solution. The higher-energy intermediate **A** is observed to couple with nitrile exclusively, implying that the reductive coupling step is under kinetic control and the resultant product distribution is governed only by the relative concentrations of nitrile and ketone. On the other hand, the reaction of the more stable intermediate **E** is governed by the more thermodynamically favorable W−O interaction in **J** and forms the oxa/aza bicyclic product exclusively (vide infra), despite the difference in concentration of the two donor solvents.

The ring-expanding insertions of unsaturated hydrocarbons,[37] ketones,[38] and carbon monoxide[39] into metallacycle M−C σ bonds are well-known. Conversely, the addition of unsaturated molecules across metal−nitrogen bonds of amido complexes has been observed only in the case of CO and other compounds such as CO_2 or PhNCO that contain sites of electrophilicity.[40] To the best of our knowledge, the addition of a ketone across a metal−imide bond to form bicyclic complexes such as **9** and **10** is unprecedented. This transformation constitutes a unique sequential [2 + 2] regioselective cycloaddition of phenyl acetylene, nitrile, and acetone within the metal's coordination sphere.

C. Nitrile Addition across the W−N Bond. In the absence of an added protic source or electrophile, the blood-red products resulting from the thermolysis of 1 in MeCN or EtCN are generated in virtually quantitative yield (eq 6). These bicyclic amidinate complexes

$$1 \xrightarrow[\text{45 °C, 24 h}]{\text{RCN / -SiMe}_3} \qquad (6)$$

11 R=Me, R'=R"=H
12 R=Et, R'=H, R"=Me
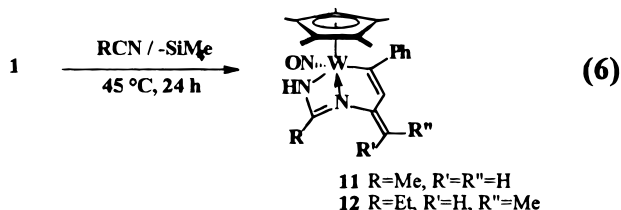
are isolable as microcrystalline solids and are air stable in solution or in the solid state for periods up to 1 month. As described for compounds **9** and **10** (vide supra), the

(36) Alías, F. M.; Belderraín, T. R.; Paneque, M.; Poveda, M. L.; Carmona, E. *Organometallics* **1997**, *16*, 301.

(37) (a) Reference 3a. (b) Tebbe, F. N.; Parshall, G. W.; Reddy, G. S. *J. Am. Chem. Soc.* **1978**, *100*, 3611. For more recent examples, see: (c) Bruck, M. A.; Copenhaver, A. S.; Wigley, D. E. *J. Am. Chem. Soc.* **1987**, *109*, 6525. (d) Christensen, N. J.; Legzdins, P. *Organometallics* **1991**, *10*, 3070. (e) Yeh, W.-Y.; Ho, C.-L.; Chiang, M. Y.; Lin, I.-T. *Organometallics* **1997**, *16*, 2698 and references therein. (f) Yang, S.-M.; Chan, M. C.-W.; Cheung, K.-K.; Che, C.-M.; Peng, S.-M. *Organometallics* **1997**, *16*, 2819.

(38) (a) Reference 26a. (b) Meinhart, J. D.; Grubbs, R. H. *Bull. Chem. Soc. Jpn.* **1988**, *61*, 171. (c) Christensen, N. J.; Legzdins, P.; Trotter, J.; Yee, V. C. *Organometallics* **1991**, *10*, 3070. (d) Buchwald, S. L.; Grubbs, R. H. *J. Am. Chem. Soc.* **1983**, *105*, 5490. (e) Yasuda, H.; Okamoto, T.; Mashima, K.; Nakamura, A. L. *Organomet. Chem.* **1989**, *363*, 61. (f) Beckhaus, R. *J. Chem. Soc., Dalton Trans.* **1997**, 1991.

(39) For a leading reference, see: Kablaoui, N. M.; Hicks, F. A.; Buchwald, S. L. *J. Am. Chem. Soc.* **1997**, *119*, 4424.

(40) See, for example: (a) Cabeza, J. A.; del Río, I.; Franco, J.; Grepioni, F.; Riera, V. *Organometallics* **1997**, *16*, 2763. (b) Cowan, R. L.; Trogler, W. C. *J. Am. Chem. Soc.* **1989**, *111*, 4750. (c) Bryndza, H. E.; Fultz, W. C.; Tam, W. *Organometallics* **1985**, *4*, 939.
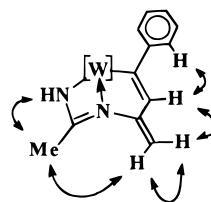

Figure 6. NOE results for the indicated environments in complex **11**. [W] represents Cp*W(NO). $\leftrightarrow$ indicates an observed NOE.

imine N atom is correctly disposed relative to the NO ligand for dative bonding to W, thus rendering **11** and **12** electronically and coordinatively saturated at the metal center.[25]

The close similarity of the bicyclic ring in these compounds to that established for the structurally characterized **10** aids in the formulation of these compounds on the basis of their spectroscopic data. Utilizing compound **11** as an example, the characteristic signals of the azametallacyclopentenyl ring components are easily identified in the NMR spectral data (Table 3). A broad singlet at 4.73 ppm in the ^{1}H NMR spectrum and a ν_{NH} at 3268 cm^{-1} in the KBr-pellet IR spectrum reveal the presence of the amine H. Likewise, the signal attributable to the resonance of the ring vinyl proton is clearly discernible at 6.83 ppm. A short-range [1]H−[13]C correlation experiment identifies the carbon signals to which the proton environments, particularly the vinyl signals, are coupled. For example, the endocyclic vinyl proton resonance at δ 6.83 couples to the carbon signal at 138.8 ppm with a coupling constant of 158 Hz, a value obtained from a gate-decoupled ^{13}C NMR experiment. Likewise, the exocyclic vinyl resonances at 4.73 and 4.45 ppm in the ^{1}H NMR spectrum couple to the carbon-13 signal at 90.6 ppm ($^1J_{CH} = 152$ Hz). Hence, the ring substituents (the vinyl H, CH_2 vinyl group, methyl substituent, and phenyl group) are identifiable from these data, although their connectivity is not. The bicyclic structure of this ring system is implied by analogy to the solid-state molecular structure determined for complex **10**, but the location of the NH, methyl, and vinyl CH_2 units can only be assigned through the combination of NOE and long-range [1]H−[13]C correlation data. The spatial arrangement of these substituents is clearly revealed by the results of an NOE experiment (Figure 6).

It, thus, remains to assign the quaternary nuclei to which these substituents are bound, utilizing the results of a HMBC [1]H−[13]C correlation experiment. Thus, both the endocyclic vinyl H signal and that of the phenyl *ortho*-H couple via a two-bond interaction to the quaternary signal at 191.9 ppm, which can be assigned as the C α to W. Likewise, the endocyclic vinyl H signal shows a two-bond coupling to the signal at 156.1 ppm, as does one of the signals attributable to the geminal vinyl protons. This signal is, therefore, attributed to the quaternary imine carbon. Both geminal vinyl proton signals couple to the endocyclic vinyl carbon signal at 138.8 ppm. Finally, the quaternary carbon signal at 171.1 ppm shows a coupling to the singlet assigned to the methyl substituent at 2.11 ppm, which permits its assignment as the quaternary amidinate carbon. Complex **12** has been characterized in an analogous manner.

Scheme 9

[W] = Cp*W(NO)

11 R = Me, R' = R" = H
12 R = Et, R' = H, R" = Me
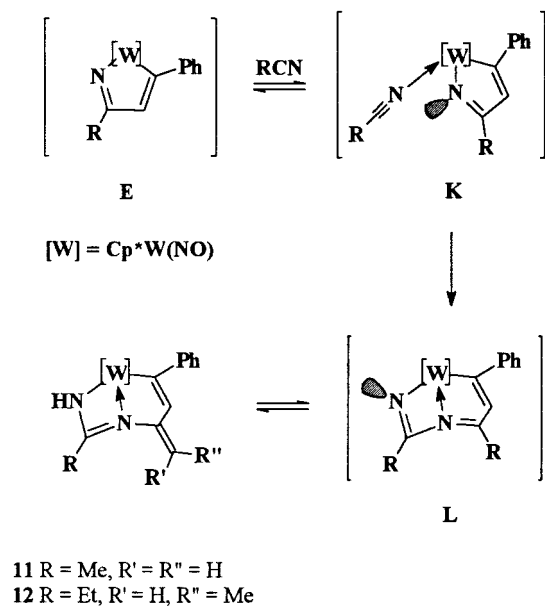
The mechanism leading to these complexes (Scheme 9) can be viewed as being analogous to that proposed for the formation of **9** and **10** (Scheme 6). The azametallacyclopentadiene **E** is first formed by reductive coupling of the acetylene and RCN at W.

A second molecule of acetonitrile coordinates (**K**) and adds across the polar W—imine link (**L**), a process facilitated by attack at the electrophilic quaternary nitrile carbon nucleus by the nucleophilic imido N in **K**. A coordinatively saturated intermediate species (**L**) is thus generated. This species, an 18e analogue of **E**, contains a basic imido N center that is quenched upon tautomerization via a formal 1,5-H shift to afford the observed products.

Interestingly, when either tBuCN, PhCN, or iPrCN is employed in this reaction, no tractable products are obtained. This is not surprising in the case of tBuCN since no product was isolated in the presence of added water either, a result that we attribute to unfavorable steric interactions between the metal complex and incoming solvent molecule, inhibiting the reductive coupling event (vide supra). In the absence of steric effects, the lack of accessible protons on the quaternary β-carbon prohibits the tautomerization step which affords the final product in these transformations. This is also the case for PhCN. In contrast, it is remarkable that no product is obtained with iPrCN since the isolation of **6** confirms that the reductive coupling event does indeed occur. On the other hand, the steric interactions limiting the scope of the ring expansion that affords complexes **9** and **10** might also play a key role in the analogous expansion involving nitriles. If so, it is of no consequence that thermolysis of **1** in anhydrous iPrCN yields no tractable products since during nitrile thermolysis in the presence of large organic carbonyls only complex **11** is obtained. Like compounds **9** and **10**, the insertion of a nitrile into a metal—N bond appears to be unprecedented, constituting a unique, regioselective coupling of 2 equiv of nitrile with phenyl acetylene to give the vinyl amidinate complexes **11** and **12**.

Several other experiments have been performed to corroborate our structural and mechanistic proposals.

For example, no ligand substitution chemistry occurs for **11** under thermolysis conditions in the presence of MeCN-d_3 and PMe$_3$.[41] This fact coupled to the absence of characteristic IR[42] and ^{13}C NMR[43] evidence suggests that the second equivalent of acetonitrile has added across the W—N linkage. A labeling study indicates that the tautomerization step is a reversible one. Thus, thermolysis of authentic **11** in THF-d_8 containing D$_2$O results in label incorporation at the amine position as well as at the exocyclic methyl position *and* the exocyclic vinyl position, thereby affording 11-d_6 but *not* facilitating the conversion of **11** to **4**-d_2. Since the intramolecular tautomerization is reversible, the ring expansion affording L must be irreversible to account for the fact that **11** is not converted to **4** in the presence of water. (This deuterated complex, **11**-d_6, can also be prepared independently by thermolysis of **1** in MeCN-d_3.) The extensive deuteration in the ring substituents of 11-d_6 leads to the conclusion that both a formal 1,3- *and* a formal 1,5-tautomerization process[44] are in operation, with the thermodynamic product resulting from a 1,5-H shift. To probe this tautomerization mechanism further, a crossover experiment involving thermolysis of an equimolar mixture of 11-d_6 and **12** in THF-d_8 was performed. Monitoring of this mixture by ^{1}H NMR spectroscopy reveals the slow incorporation of the deuterium label into the amine, ethyl, and methylvinyl susbtituents in **12** and proton incorporation into the analogous sites in 11-d_6, a clear indication of the *intermolecular* nature of this tautomerization process.[45] A striking feature of this experiment is the slow rate of conversion. After 24 h at 65 °C, the deuterium scrambling is approximately 50% complete, as judged by integration of the methyl signals at about 2.1 and 1.3 ppm in the ^{1}H NMR spectrum. Since the thermolyses to form complexes **2**−**12** require approximately 24 h at 45 °C, both the dilute concentration of the NMR sample and an isotope effect presumably retard the rate of tautomerism in this experiment, a conclusion fully in accord with the proposed bimolecular mechanism.[46]

The competition by MeCN and water for reaction with intermediate **E** has been tested by conducting the thermolysis of **1** in MeCN containing 2, 5, and 10 equiv of water ([H$_2$O] = 19, 46, and 93 mM, respectively). Formation of **11** (~5%) was observed only in the case where [H$_2$O] = 19 mM, as detected by ^{1}H NMR spectroscopy of the three mixtures after their thermolysis for 24 h. Quantitative conversion to **4** was indicated in the ^{1}H NMR spectra of the final mixtures in the latter two cases. Thus, the ring expansion afforded by the insertion of a second acetonitrile molecule must be a more energetically demanding process; only at very low water concentrations does this process become competitive with protonation of **E** by water.

(41) Legzdins, P.; Sayers, S. F. *J. Am. Chem. Soc.* **1994**, *116*, 12105.
(42) Nakamoto, K. *Infrared and Raman Spectra of Inorganic and Coordination Compounds*, 4th ed.; Wiley-Interscience: New York, 1986.
(43) Yeh, W.-Y.; Ting, C.-S.; Chih, C.-F. *J. Organomet. Chem.* **1991**, *427*, 257.
(44) The formal 1,5-tautomerization can also be viewed as two sequential 1,3-H shifts; the first transfer occurs from the methyl group to the internal imine N and the second from the internal imine N to the terminal amide N. That the tautomerization is shown to be intermolecular renders these labels formal descriptors only.
(45) For an elegant kinetic and mechanistic study of an analogous intermolecular tautomerization process in (DIPP)$_3$Ta(η^2-HNC(=CH$_2$)C-(Ph)=CPh) , see ref 26c.
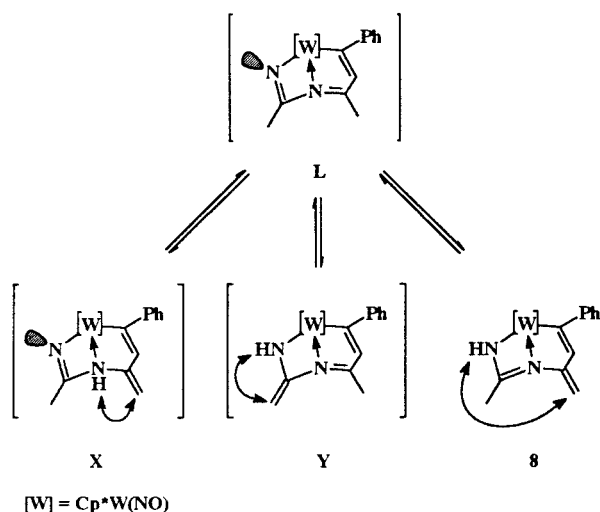
Figure 7. Possible tautomeric pathways affording 18e complexes from intermediate **L**.

Analogous to fulvene formation in complex **8**, the extensive conjugation upon tautomerization undoubtedly provides the stabilization necessary for the formation of the less-stable enamine tautomer **11** under thermodynamic conditions. That an intermolecular proton shift from the internal Me substituent to the terminal imido N results in the exclusive formation of **11** as the thermodynamic product can be rationalized (Figure 7) by considering conjugation effects and orbital overlap arguments analogous to those presented for **E**. As noted previously (Scheme 9), the internal imido N is properly oriented for dative bonding to W in both **L** and **11**, thereby conferring a closed-shell electronic configuration on both of these complexes. That **L** proceeds to abstract a proton intermolecularly is an indication of the basic nature of the terminal imido N. On the other hand, the internal imido N is reduced in its Lewis basicity as a result of coordination to W; a proton transfer affording the internal amine (**X**) is therefore improbable. Such a shift would also lead to a disruption of the ring conjugation, again yielding the thermodynamically least-stable tautomer of the three. On the other hand, the formation of both **Y** and **11** result in substantial ring conjugation, and yet **11** is the only thermodynamic product observed. The relative stability of **11** over **Y** is probably a result of the formation of the more stable amidinate unit in the conjugated backbone in **11**.[47]

Kinetic Studies. The fact that the conversions described in this paper are very clean prompted us to consider furthering our understanding of this chemistry through kinetic studies. UV−vis spectroscopy was employed as the method of choice for collecting well-defined kinetic data. Quantification of these data is effected by monitoring the growth of the shoulder at 336 or 350 nm, the results of which are summarized in Table 5. The conversions of complex **1** to **11**, **4**, and **3** under thermolysis conditions at 45 °C were monitored in this way, and the observed rate constants were determined from a first-order analysis of the data.

The mechanism originally proposed[7] to account for the observed C−H activation of *n*-pentane and *n*-hexane emphasized an initial elimination of SiMe$_4$ from **13** to

Table 5. Kinetic Data for the Conversion of 1 to 11, 4, and 3

solvent	temp (K)	[H$_2$O] (M)	product complex	k_{obs} ($\times 10^{-5}$ s^{-1})	R^2	av k_{obs} ($\times 10^{-5}$ s^{-1})
MeCN	318		**11**	4.9	0.9994	
MeCN	318		**11**	4.7	0.9994	4.7 ± 0.2
MeCN	318		**11**	4.5	0.9997	
MeCN	318	0.12	**4**	4.5	0.9996	
MeCN	318	0.12	**4**	4.7	0.9997	4.6 ± 0.1
MeCN	318	0.06	**4**	5.0	0.9998	
MeCN	318	0.06	**4**	4.4	0.9998	4.6 ± 0.4
MeCN	318	0.06	**4**	4.5	0.9999	
MeCN	318	0.03	**4**	4.5	0.9999	
MeCN	318	0.03	**4**	4.6	0.9997	4.6 ± 0.1
MeCN	318	0.03	**4**	4.8	0.9998	
MeCN	318	0.006	**4**	4.4	0.9997	
MeCN	318	0.006	**4**	4.7	0.9983	4.7 ± 0.3
MeCN	318	0.006	**4**	4.9	0.9998	
EtOAc	318		**3**	2.8	0.99996	
EtOAc	318		**3**	3.0	0.9998	2.9 ± 0.1
EtOAc	318		**3**	3.0	0.9997	
EtOAc	327		**3**	9.7	0.9998	
EtOAc	327		**3**	11	0.99992	10 ± 1
EtOAc	336		**3**	51	0.99996	
EtOAc	336		**3**	49	0.9997	50 ± 1
EtOAc	341		**3**	90	0.9997	
EtOAc	341		**3**	93	0.9996	95 ± 6
EtOAc	341		**3**	103	0.9994	
EtOAc	348		**3**	265	0.9996	
EtOAc	348		**3**	268	0.9996	276 ± 16
EtOAc	348		**3**	295	0.9998	

produce the η^2-acetylene intermediate **A**.[48] We propose here a rate-limiting generation of **A** through an E1-type dissociation pivotal to the mechanisms giving rise to both modes of reactivity. The results outlined in Table 5 support the proposed rate-limiting generation of η^2-acetylene intermediate **A** in all of these reactions and mitigate against an alternative bimolecular S$_N$2-type associative mechanism; in such a case, a significant rate dependence on the nature of the incoming substrate would be expected.[49] Hence, the rates of conversion of **1** in acetonitrile doped with water afford observed rate constants from 4.6×10^{-5} s^{-1} to 4.7×10^{-5} s^{-1} for water concentrations ranging from 0.006 to 0.12 M, eliminating the possibility of a bimolecular saturation mechanism involving hydration of azametallacycle **E** by water. More importantly, the rates of conversion of **1** in the presence of different substrates are remarkably similar, ranging from 2.98×10^{-5} s^{-1} to 5.04×10^{-5} s^{-1}. The slight variance in the observed rate constants for the formation of **11**, **4**, and **3** can be ascribed to the differences in the bulk properties of the solvents and not to any definable mechanistic differences.[50] A study of the temperature dependence of the reaction rate (Figure 8) yields an enthalpy and entropy of activation of 32(3) kcal mol^{-1} and 21(2) cal (mol·K)$^{-1}$, respectively. The magnitude of the enthalpy reflects considerable

(46) The results of this crossover experiment only confirm the intermolecular component to this tautomerization. An intramolecular component cannot be ruled out in the absence of the appropriate kinetic studies.

(47) A very rapid isomerization (on the NMR time scale) between Y and **11** cannot be discounted from the experimental data.

(48) A manuscript describing the scope of the thermal C−H activation chemistry observed for this system in the presence of a variety of hydrocarbons, including a detailed kinetic and mechanistic analysis, is currently in preparation.

(49) Carmona proposes such a mechanism for the formation of an analogous iridapyrrole complex: see ref 23a.

(50) Connors, K. A. *Chemical Kinetics: The Study of Reaction Rates in Solution;* VCH Publishers: New York, 1990; Chapter 8.
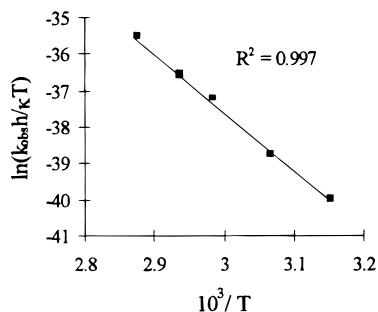
Figure 8. Eyring plot for the thermolysis of **1** in EtOAc, $308 < T < 348$ K.

bond scission at the transition state, while the small and positive value of the activation entropy implies a degree of dissociative character in the rate-limiting step. Comparable findings have been reported for a similar rate-limiting reductive elimination process.[51]

Ring Expansion and Ligand Elaboration. In Schemes 5, 8, and 9 we propose that the chemistry leading to complexes **4**–**12** arises from the specific incapability of the N atom in intermediate **E** to function as a 3e donor to W, an effect caused by the conformational restrictions of the metallacycle. Two salient consequences of this are (i) the electronic unsaturation of the metal center in these intermediate complexes and (ii) the resultant basicity or nucleophilicity conferred on the imido N which affords a reactivity beyond the initial reductive coupling event. The origin of these chemical characteristics in the azametallacycle **E** (and also in the O-containing analogue **C**) deserves further discussion in light of the fact that the analogous complexes for the Cp_2Zr system are readily isolated and have been extensively studied. In addition to the greater oxophilicity of the group 4 metals being a stabilizing influence in these metallacycles, an orbital-overlap argument can also be made for the differences in reactivity. Such a rationale requires a brief review of the Lewis acidity inherent to the 16e model complexes $CpM(NO)Me_2$ (M = Mo, W). It has been demonstrated computationally[52] that there exists a metal-centered d_{xy}-type LUMO in these complexes oriented perpendicular to the M–NO vector, with the most sterically accessible lobe bisecting the R–W–R angle (Figure 9, case I).

Furthermore, it has been shown experimentally[53] that 16e bis(alkyl) complexes of type I are Lewis acidic and that the coordination of 2e Lewis bases occurs cis to both alkyl ligands at the most kinetically accessible lobe of the LUMO.[54] Thus, it is a reasonable assumption that a similar metal-centered LUMO exists in the related complexes containing an NR_2 or OR ligand (case II, NR_2 ligand depicted). Here, however, the heteroatom-containing ligand can orient to stabilize the metal-centered LUMO through donation of electron density
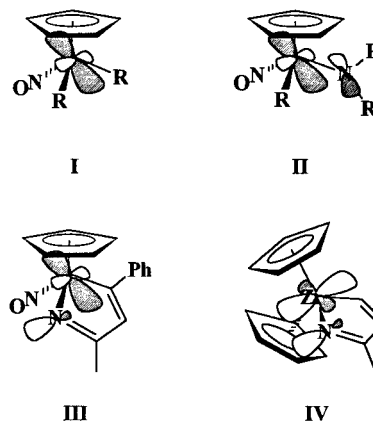
(51) Buchanan, J. M.; Stryker, J. M.; Bergman, R. G. *J. Am. Chem. Soc.* **1986**, *108*, 1537.
(52) (a) Legzdins, P.; Rettig, S. J.; Sánchez, L. J.; Bursten, B. E.; Gatter, M. G. *J. Am. Chem. Soc.* **1985**, *107*, 1411. (b) Bursten, B. E.; Cayton, R. H. *Organometallics* **1985**, *6*, 2004.
(53) (a) Legzdins, P.; Rettig, S. J.; Sánchez, L. J. *Organometallics* **1988**, *7*, 2394. (b) Reference 25. (c) Legzdins, P.; Veltheer, J. E. *Acc. Chem. Res.* **1993**, *26*, 41.
(54) The other three lobes of the LUMO are kinetically inaccessible. One of the three extends upwards toward the Cp* ring, whereas access to the other two lobes is presumably blocked by the Cp* methyl substituents (which have been omitted for clarity in Figure 9).

Figure 9. Frontier orbitals in isolobal CpW(NO) (**I**–**III**) and Cp_2Zr (**IV**) complexes.

from the N p-type filled orbital into this orbital, yielding an 18e, saturated metal center. This phenomenon is reflected structurally in the coplanarity of the W–NO and the N–R or O–R vectors in the molecular structures determined for such compounds[55] and is supported by computational modeling.[14] In the case of intermediate **E**, however, the filled orbital on N is forced to point away from the metal center by the conformation of the ring (case III). Reduced orbital overlap occurs, which, in combination with the diminished oxophilicity of W relative to Zr, leads to an increase in the Lewis basicity of the imido N and Lewis acidity of the metal center. In comparison, the analogous LUMO in the zirconocene system contains two disproportionately larger lobes.[56] These larger, more accessible lobes are exterior to the azametallacycle, one being adjacent to the imide N, making donation from the filled N orbital into this LUMO facile (case IV). Thus, complexes of this type are stabilized for the group 4 case and are readily isolable. That a kinetic opportunity exists for the addition of ROH, ketones, or nitriles across the W–N bond in intermediate **E** we propose to be a consequence of the greater electron density at the imide N in addition to the reduced steric requirements of the NO ligand. The analogous chemistry is not observed in the isolobal zirconocene system, despite the fact that small molecules such as H_2O and CO react with the zirconocene analogues to release the ring from the metal center. The smaller metallocene wedge in the latter system probably offers little opportunity for reaction with larger, unsaturated heteroatom-containing molecules at the metal center once the products of reductive coupling have formed.

Epilogue

In this paper, the products of the reductive coupling of esters and nitriles with coordinated phenyl acetylene in the coordination sphere of the Cp*W(NO) template are described. Driving the chemistry that occurs beyond the reductive coupling event is the inability to attain an 18e configuration at the W center, a feature in contrast to previously published work involving the isolobal zirconocene system. A number of pathways are

(55) (a) Kuzelka, J.; Legzdins, P.; Rettig, S. J.; Smith, K. M. *Organometallics* **1997**, *16*, 3569.
(56) Lauer, J. W.; Hoffmann, R. *J. Am. Chem. Soc.* **1976**, *98*, 1729.

employed by the Cp*W(NO)(η^2-PhC≡CH) fragment in accomplishing this end. In the case involving reductive coupling to esters, β-C−O bond cleavage in the putative 16e intermediate oxametallacyclopentene complex affords alkoxide-containing, 18e oxametallacyclopentadiene complexes. In nitrile solvent, the proposed 16e azametallacyclopentadiene complex is trapped by protonation of the basic imine N by water, allyl alcohol, or CpH. Coordination of the conjugate base, thus, fulfills the electronic requirements of the metal, yielding 18e compounds. In the latter case, the tautomeric aminopentafulvene ligand is formed which exhibits interesting fluxional behavior at room temperature in solution. In the presence of acetone, the intermediate azametallacyclopentadiene complex is trapped by a chemo- and regioselective ring-expanding addition of ketone. In the absence of any trapping agent, a second equivalent of RCN inserts in a manner analogous to acetone, an intermolecular proton shift affording the observed vinyl amidinate complex. A kinetic study of these transformations implicates a mechanism involving rate-limiting elimination of SiMe₄ from the parent bis(hydrocarbyl) complex. In all cases studied, reaction ensues beyond the initial reductive coupling event until electron saturation of the metal center is achieved. This phenomenon has been rationalized through a qualitative discussion of frontier orbitals; a reduced compatibility of the heteroatom lone-pair orbital(s) with the metal-centered LUMO in the proposed 16e transient W species results in a Lewis-acidic metal center and nucleophilic heteroatom. This incompatibility is in direct contrast to the 18e configuration achievable by the analogous zirconocene system and reflects the difference in the electronic structure and oxophilicity of the two systems. The scope of the reactivity that results is an extension of, and provides an interesting contrast to, the body of work surrounding the analogous zirconocene system.

Experimental Section

General Methods. All reactions and subsequent manipulations were performed under anaerobic and anhydrous conditions using an atmosphere of dinitrogen or argon. General procedures routinely employed in these laboratories have been described in detail previously.[57] The organometallic reagent Cp*W(NO)(CH₂SiMe₃)(CPh=CH₂) (1) was prepared according to the reported procedure.[7] Ethyl acetate, methyl acetate, acetonitrile, propionitrile, isobutyronitrile, *tert*-butyl nitrile, benzonitrile, and allyl alcohol (Aldrich) were distilled or vacuum-transferred from CaH₂. Acetone was refluxed over Linde 4A molecular sieves, distilled onto vigorously anhydrous Linde 4A molecular sieves, and vacuum-transferred as needed. CpH was cracked from cyclopentadiene dimer and stored cold in the dark under an inert atmosphere. Wet acetonitrile was prepared by deaerating HPLC-grade solvent obtained directly from Aldrich or by adding microliter amounts of distilled, deionized water to rigorously dried acetonitrile via a microsyringe. Acetonitrile-d_3 (CIL) was dried over CaH₂ and vacuum-transferred. Deuterated water (CIL) was deaerated under a flow of argon immediately prior to use. Spectroscopic data, yields, and elemental analyses of all new complexes synthesized during this work are collected in Tables 1−3. Where appropriate, NOE, HMQC, HMBC, and gate-decoupled ¹³C experiments were performed on a Bruker AMX 500 MHz NMR spectrometer to facilitate ¹H and ¹³C spectral assignments.

Kinetic Studies. Kinetic studies were performed using a HP8452 UV−vis spectrometer equipped with a thermostated cell holder connected to a VWR 1150 constant-temperature bath which was accurate to ±0.25 °C. Typical kinetic runs monitored the product band at 336 or 360 nm arising from the thermolysis of 0.1−1 mg of **1** dissolved in 3 mL of solvent over not less than 3.5 half-lives. Absorbance values for t_∞ were obtained by computer optimization of the squared residual, R^2, for the regression line fitted to the data through a first-order analysis.

X-ray Diffraction Studies. Data collection and structure solution for complexes **2**, **4**, **8**, and **10** were conducted at the X-ray Crystallographic Laboratory at the University of Minnesota. All calculations were performed using SGI Indy RR4400-SC or Pentium computers using the SHELXTL V5.0 suite of programs.

A crystal of each compound was attached to a glass fiber and mounted on a Siemens SMART system for data collection at 173(2) K. An initial set of cell constants was calculated from reflections harvested from three sets of 20 frames. Final cell constants were calculated from sets of strong reflections obtained during the actual data collection. Crystallographic data are presented in Table 4. In the hemisphere collection technique employed during this work, a randomly oriented region of reciprocal space was surveyed to the extent of 1.3 hemispheres to a resolution of 0.84 Å. Three major swaths of frames were collected with 0.30° steps in ω. This collection strategy provided a high degree of redundancy in the data as well as providing good ψ input in the event that an empirical absorption correction had to be applied. The space groups were determined based on systematic absences and intensity statistics. In each case, a successful direct-methods solution was calculated which provided most non-hydrogen atoms from the *E*-map. Several full-matrix least-squares difference-Fourier cycles were performed which located the remainder of the non-hydrogen atoms. All non-hydrogen atoms were refined with anisotropic displacement parameters unless stated otherwise. All hydrogen atoms were placed in ideal positions and were refined as riding atoms with individual or relative isotropic displacement parameters.

The refinement of the data collected for complex **2** was hampered by twinning in the crystal, as evinced by an R1 of 7.2% and a list of 50 worst reflections containing largely $h = 4$ reflections. A successful attempt was made to locate enough reflections of the twin to index it; the twin law thus determined is (by rows) 100, 0,−1,0, −³/₄,0,1, which explains why all $h = 4$ reflections have $F_o^2 \gg F_c^2$. The program UNTWIN[58] was used to create a HKLF 5-type reflection file from the original HKLF 4 file. No data from the minor twin were used to create the new reflection file. The residual improved 2%, and all atoms became positive definite. The twin is ~19% of the mass of the main specimen.

Preparation of Cp*W(NO)(OMe)(η^2-*O*=C(Me)CH=*C*Ph) (2). Cp*W(NO)(CH₂SiMe₃)(CPh=CH₂) (**1**, 135 mg, 0.25 mmol) was dissolved in MeOAc (10 mL) in a thick-walled bomb. The resulting deep red solution was heated at 45 °C for 24 h, during which time its color changed to purple. Solvent was removed from the final solution in vacuo, and the purple residue was extracted with a minimum of a CH₂Cl₂/hexanes mixture (1:1). The extract was filtered through a plug of Celite (1.5 × 0.5 cm) supported on a frit, and the volume of the filtrate was reduced in vacuo. Cooling the concentrated solution to −30 °C overnight induced the deposition of dark purple needles of complex **2** (89 mg), which were isolated by removal of the supernatant solution. A second crop of crystals (28 mg) was obtained by reducing the volume of the supernatant solution and cooling for a further 24 h.

(57) Legzdins, P.; Rettig, S. J.; Ross, K. J.; Batchelor, R. J.; Einstein, F. W. B. *Organometallics* **1995**, *14*, 5579.

(58) Young, V. G., Jr., *UNTWIN*; X-ray Crystallographic Laboratory, Chemistry Department, The University of Minnesota: Minneapolis, MN, 1997.

Preparation of Cp*W(NO)(OEt)(η^2-*O*=C(Me)CH=*C*Ph) (3). Complex **3** was prepared in a manner analogous to that described in the preceding paragraph for **2**. After having been heated for 24 h, the reaction mixture was reduced in volume and the burgundy solution was cooled to −30 °C overnight to induce the deposition of **3** as analytically pure needles (112 mg), which were isolated by removal of the supernatant solution and subsequent drying under vacuum.

Preparation of Cp*W(NO)(OH)(η^2-H*N*=C(Me)CH=*C*Ph) (4). Reactant **1** (135 mg, 0.25 mmol) was dissolved in wet MeCN (10 mL) in a thick-walled bomb. The solution was heated for 24 h at 45 °C, whereupon it became light orange in color and a red crystalline solid deposited in the bottom of the bomb. The orange supernatant solution was removed by pipet, and the crystals were dried under vacuum. The supernatant solution was filtered through a Celite plug (1.5 × 0.5 cm), and the volume of the filtrate was reduced in vacuo. The resulting dark orange solution was then cooled to −32 °C overnight to induce the deposition of a second fraction of **4** as orange microcrystals (107 mg), which were isolated as described above.

Preparation of Cp*W(NO)(OD)(η^2-D*N*=C(Me)CH=*C*Ph) (4-d_2). Complex **4**-d_2 was prepared in a manner similar to that employed for **4** (vide supra), except that reactant **1** (135 mg, 0.25 mmol) was first dissolved in dry MeCN (10 mL) and the red solution was then doped with D_2O (25 μL, 1.4 mmol). After thermolysis, the dark orange solution was concentrated and cooled to induce crystallization. Red crystalline **4**-d_2 was isolated by removal of the solvent and washing with Et_2O. This complex was characterized by EI-MS and by comparison of its ^{1}H NMR spectroscopic properties to those displayed by **4**.

Preparation of Cp*W(NO)(OH)(η^2-H*N*=C(Et)CH=*C*Ph) (5) and Cp*W(NO)(OH)(η^2-H*N*=C(^{i}Pr)CH=*C*Ph) (6). Both complexes **5** and **6** were prepared in a manner similar to that employed for **4**. Following the thermolyses, the final reaction mixtures were concentrated and cooled to −32 °C overnight to induce the deposition of **5** as red needles (82 mg) and **6** as red blocks (87 mg). Further concentration and cooling of the supernatant solutions afforded second crops of the products (18 mg of **5** and 25 mg of **6**), which were isolated by removal of the mother liquor and drying under vacuum.

Preparation of Cp*W(NO)(OCH₂CH=CH₂)(η^2-H*N*=C-(Me)CH=*C*Ph) (7). Complex **7** was prepared in a manner identical with that for **5**, except that allyl alcohol (280 μL, 16 equiv) was added via microsyringe in place of the water. The final dark orange solution was concentrated and cooled twice to obtain red needles of **7** in two crops (78 and 33 mg). The crystals were isolated and dried in the usual fashion.

Preparation of Cp*W(NO)(HNC(=C(C₄H₄))(Me))(η^2-*N*H=C(Me)CH=*C*Ph) (8). Complex **8** was prepared in a manner identical with that for **5**, except that excess CpH was added via syringe in the place of water. The thermolyzed dark red solution was concentrated and cooled to obtain **8** as dark red needles (112 mg) after isolation and drying under high vacuum.

Preparation of Cp*W(NO)(η^3-*O*C(Me)₂*N*=C(Me)-CH=*C*Ph) (9). Complex **9** was prepared in a manner identical with that for **8**, except that excess acetone was added by vacuum transfer onto a frozen MeCN solution of **1** (135 mg, 0.25 mmol). After thermolysis, the resultant red-brown solution was concentrated and cooled to obtain **9** as brown irregular blocks (99 mg) after isolation and drying under high vacuum.

Preparation of Cp*W(NO)(η^3-*O*C(Me)₂*N*=C(^{i}Pr)-CH=*C*Ph) (10). Complex **10** was prepared in a manner analogous to that for **9**. and was isolated in two crops as brown-red blocks (102 mg) by concentration and cooling of the final reaction mixture.

Preparation of Cp*W(NO)(η^3-H*N*C(Me)=*N*C(=CH₂)-CH=*C*Ph) (11). Reactant **1** (270 mg, 0.5 mmol) was dissolved in MeCN (20 mL) in a thick-walled bomb, and the solution was heated for 24 h at 50 °C. The final blood-red solution was

taken to dryness under reduced pressure, and the residue was triturated with pentane (3 × 5 mL), washed with Et_2O (3 × 5 mL) and dried under high vacuum. The remaining solid was dissolved in a minimum volume of CH_2Cl_2/hexanes (1:1), and the solution was filtered through Celite (1 × 2 cm plug). The filtrate was reduced in volume and cooled to −32 °C overnight. Complex **11** was isolated the next day as a dark red microcrystalline powder (207 mg) after removal of the supernatant solution and drying under vacuum.

Preparation of Cp*W(NO)(η^3-D*N*C(CD₃)=*N*C(=CD₂)-CH=*C*Ph) (11-d_6). Complex **1** (30 mg, 0.056 mmol) was dissolved in MeCN-d_3 (0.5 mL) in an NMR tube and was heated at 45 °C for 24 h. The solvent was then removed in vacuo, and the red solid was washed twice with Et_2O and dried under high vacuum for 4 h. Characterization of **11**-d_6 was effected by EI-MS and by comparison of its ^{1}H NMR spectrum (CDCl₃) to that exhibited by **11**.

Preparation of Cp*W(NO)(η^3-H*N*C(Et)=*N*C(=CHMe)-CH=*C*Ph) (12). Complex **12** was prepared in a manner identical with that for **11**, except that the dark red-brown solution produced by thermolysis was reduced in volume and cooled overnight twice to induce the deposition of two crops of **12** (96 mg total) as brown, analytically pure microcrystals.

Reaction of 4 with D₂O. Complex **4** (20 mg, 0.040 mmol) was dissolved in MeCN-d_3 (0.5 mL) in an NMR tube, and D_2O (10 μL, 0.56 mmol) was added. The resulting solution was heated at 45 °C overnight, and its ^{1}H NMR spectrum was then recorded. Quantitative formation of **4**-d_2 was indicated by a comparison of this spectrum to that exhibited by an authentic sample of **4**-d_2.

Thermolysis of 4 in EtOAc. Complex **4** (20 mg, 0.040 mmol) was dissolved in EtOAc (3 mL) in a glass bomb and heated for 24 h at 45 °C. The volatiles were removed under vacuum after cooling the orange solution. Comparison of the ^{1}H NMR spectrum (CDCl₃ solution) of the resultant orange solid to that of authentic **4** indicated no reaction during thermolysis in EtOAc.

Thermolysis of 7 in CD₃NO₂ containing D₂O. Complex **7** (15 mg) was dissolved in CD₃NO₂, and D_2O (2 μL) was added. After thermolysis at 50 °C for 16 h, the ^{1}H NMR spectrum of the mixture was recorded. Signals attributable to **4**-d_2 and free allyl alcohol indicated partial conversion. Further heating for an additional 72 h resulted in ~35% conversion to **4**, as evinced in the ^{1}H NMR spectrum of the solution.

Thermolysis of 9 in THF-d_8 containing D₂O. Complex **9** (15 mg) was dissolved in THF-d_8, and D_2O (2 μL) was added to the solution. After thermolysis at 50 °C for 16 h, the ^{1}H NMR spectrum of the mixture was recorded. Only signals attributable to **9** were evident, indicating no conversion to **4**-d_2.

Thermolysis of 1 in MeCN containing 2, 5, and 10 equiv of H₂0. Reactant **1** (30.0 mg, 55.6 μmol) was dissolved in dry MeCN (6.0 mL), and the resulting solution was divided into three 2-mL aliquots which were placed into three glass bombs. Two, five, and ten equivalents of water (0.7, 1.7, and 3.5 μL) were added to the first, second, and third bombs, thereby affording solutions with $[H_2O]$ = 19, 47, and 95 mM, respectively. Following thermolyses at 45 °C for 24 h, the volatiles were removed from the final mixtures under high vacuum and the red-orange residues were taken up in CDCl₃ (0.5 mL). The ^{1}H NMR spectra of the three resulting solutions were recorded and compared to the ^{1}H NMR spectrum (CDCl₃) of an equimolar mixture of authentic **11** and **4**, revealing that in only the case where $[H_2O]$ = 19 mM was **11** observed to form, in approximately 5%. The formation of **4** was quantitative for $[H_2O]$ ≥ 47 mM.

Thermolysis of 11 in THF-d_8 containing D₂O. An excess of D_2O was added via microsyringe to a solution of pure **11** dissolved in THF-d_8. The solution was placed in a thermostated water bath at 55 °C, and its ^{1}H NMR spectra were recorded at regular intervals over a 48 h period. The resulting

spectra revealed quantitative conversion to **11**-d_6 by comparison to the proton spectra of authentic **11** and **11**-d_6.

Thermolysis of 11-d_6 and 12 in THF-d_8. The crossover experiment involving equimolar amounts of **11**-d_6 and **12** dissolved in THF-d_8 was performed. An initial ^{1}H NMR spectrum was recorded, and the solution was then placed in a 65 °C oil bath for 72 h, during which time its ^{1}H NMR spectra were recorded at regular intervals. The progress of the experiment was followed by comparison of the resultant spectra to those for authentic **11** and **12** and revealed an intermolecular exchange process between the acidic sites in the two compounds.

Supporting Information Available: Thermal ellipsoid plots for compounds **2**, **4**, **8**, and **10** (Figures S1−S4) and tables listing full crystallographic information, atomic coordinates and U_{eq}, anisotropic thermal parameters, intramolecular bond distances and angles (Tables S1−S24), and full NMR data (Table S25) (39 pages). Ordering information is given on any current masthead page.

OM971080R